2025 Southeastern Region of the Society of Toxicology Fall Meeting Program

Hosted by: Clemson University

October 10, 2025

Index

Sponsors:

UL Research Institutes | Chemical Insights

Department of BIOLOGICAL SCIENCES Clemson University

College of SCIENCE

Welcome Message from SESOT President, Kylie Rock!

The SESOT Executive Committee is delighted to welcome you all to the 2025 Fall Annual Meeting of the Southeastern Regional Chapter of the Society of Toxicology, hosted this year by Clemson University!

It is an honor to host our vibrant regional community here in the Upstate of South Carolina. We're thrilled to see continued growth and engagement across our membership, with attendees and presenters joining us from Clemson University, Auburn University, the University of Georgia, the University of Florida, the University of Alabama at Birmingham, Emory University, and King University.

This year's meeting promises a full and exciting program highlighting the diverse and dynamic work being done by toxicologists across all career stages. From our keynote lecture by Dr. Sarah White and the interactive career panel to postdoctoral and graduate platform sessions and undergraduate and trainee poster presentations, the agenda is designed to showcase innovative science, spark collaboration, and strengthen professional connections across our community.

We are especially proud of our trainees, the future of toxicology, who will present their research in platform and poster competitions. These sessions continue to be a cornerstone of our meeting, offering invaluable experience and opportunities for feedback and recognition.

We would like to extend a huge thank you to our sponsors, the Chemical Insights Research Institute, the Clemson University College of Science, and the Clemson University Department of Biological Sciences, without whom this meeting would not be possible. Their generous support helps sustain our mission to foster collaboration, advance research, and provide meaningful professional development opportunities across the field of toxicology.

As we gather in person once again, I encourage you to take advantage of every opportunity to connect, collaborate, and celebrate the many facets of toxicology represented here today. Whether you're sharing your latest findings, seeking mentorship, or exploring new directions for your research, this meeting is a space for inspiration and shared purpose.

On behalf of the entire **SESOT Executive Committee**, thank you for being here and for contributing to another successful annual meeting. I hope you enjoy the day's events, the camaraderie of our community, and all that Clemson has to offer.

Warm regards,

Kylie Rock

Kylie D. Rock, Ph.D.
President, Southeastern Regional Chapter of the Society of Toxicology

P.S. If you're looking for ways to get more involved with SESOT, consider volunteering to serve as an officer, we'd love to have you join us!

Sponsors:

UL Research Institutes | Chemical Insights

Department of BIOLOGICAL SCIENCES Clemson University

College of SCIENCE

SESOT Meeting Agenda

SESOT Annual Meeting, 2025, Clemson University		
Thursday October 9th, 2025		
Welcome Reception	6:00 – 8:00pm	**Kite Hill Brewing Co.** *150 Thomas Green Blvd* Clemson, SC 29631
Friday October 10th, 2025		
Networking Breakfast & Registration	8:00 – 9:00am	**Clemson University Conference Center & Inn** Ballroom A *240 Madren Center Drive* *Clemson, SC 29634*
Welcome Remarks	9:00 – 9:15	Auditorium Dr. Kylie Rock *Clemson University*
Postdoc Platform Session	9:15 – 9:30	Dr. Nilda Sanchez, *University of Alabama at Birmingham*
Graduate Student Platform Session	9:30 – 10:30	Morgan Jacobellis, *MS Student, Clemson University* Xinyue Chen, *PhD Student, University of Florida* Syed Ferdous, *PhD Student, Clemson University* Trevor Kalinowski, *PhD Student, University of Georgia*
Morning Break	10:30 – 10:45	
Keynote	10:45 – 11:45	Dr. Sarah White, *Clemson University*
Lunch	11:45 – 12:30pm	Ballroom A
Career Panel	12:30 – 1:45	Auditorium Dr. Jay Stallons, Principal and Founder, *Tiresias Consulting* Dr. Erica Rogers, Senior Toxicologist II, *Gad Consulting Services* Dr. Lauren Wills, Associate Professor, *Charleston Southern University* Dr. Xiaojia He, Senior Research Scientist, *Research Institutes' Chemical Insights* Dr. Kylie Rock, Assistant Professor, *Clemson University*
Afternoon Break 1	1:45 – 2:00	
Poster Session	2:00 – 3:45	Ballroom A Evens from 2:00 – 2:45, Odds from 3:00 – 3:45 Poster Session Networking Bingo
Afternoon Break 2	3:45 – 4:00	
Awards and Closing Remarks	4:00 – 4:30	Auditorium

Sponsors:

UL Research Institutes | Chemical Insights

Department of BIOLOGICAL SCIENCES Clemson University

College of SCIENCE

SESOT Executive Committee 2025 – 2026

Kylie Rock
President

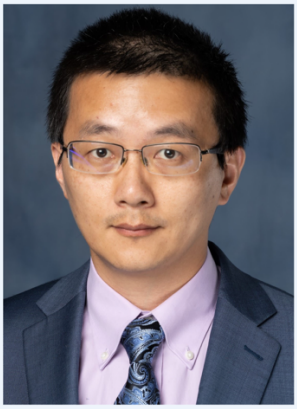

Zhoumeng Lin
President - Elect

Katharine Horzmann
Past President

Priscila Falagon Lotsch
Councilor

Natalie Gassman
Councilor

Jay Stallons
Secretary/Treasurer

Abner Nunes
Postdoctoral Representative

Ashley Adamson
Graduate Student Representative

Sponsors:

UL Research Institutes | Chemical Insights

Department of BIOLOGICAL SCIENCES Clemson University

College of SCIENCE

2025 SESOT Meeting Map

2025 SESOT Venue

Meeting Location
Clemson University Conference Center & Inn
240 Madren Center Drive
Clemson, SC 29634

Welcome Reception
Kite Hill Brewing Co.
150 Thomas Green Blvd.
Clemson SC, 29631

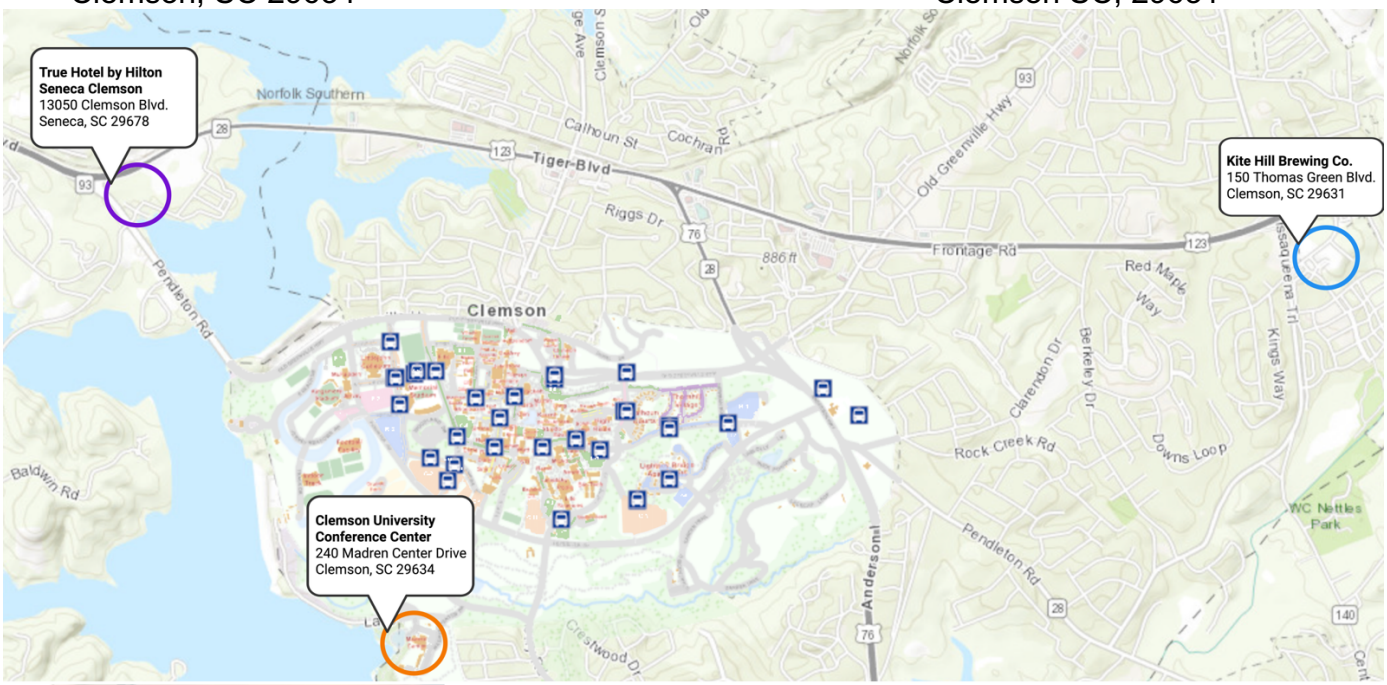

Sponsors:

UL Research Institutes | Chemical Insights

Department of BIOLOGICAL SCIENCES Clemson University

College of SCIENCE

Keynote Speaker and Panelists

Keynote Speaker

Got Plants? Low-energy environmental mitigation strategies
Sarah White, Ph.D.
Professor
Clemson University
Dr. Sarah White is a Professor in the Department of Plant and Environmental Sciences and the Nursery Extension Specialist at Clemson University. Sarah has 15+ years of experience developing and optimizing nature-based treatment technologies to clean water. Her lab is currently investigating the applications of vegetation-based technologies (constructed wetlands, floating treatment wetlands, and vegetated buffers) for cleansing agrichemical and plant disease contaminants from production runoff to encourage water reuse and conservation and evaluating reservoir design and management to enhance water security.

Career Panelists

Jay Stallons, PhD DABT
Principal and Founder
Tiresias Consulting, LLC
Jay Stallons is a board-certified toxicologist and independent nonclinical toxicology consultant in the biotechnology and animal health industries. He is the founder and principal at Tiresias Consulting, LLC where he supports clients from startups to big pharma in nonclinical development of AAV gene therapies and new veterinary drugs. Prior to starting his own firm in 2023, Jay was Associate Director of Nonclinical Safety Evaluation at Sangamo Therapeutics where he was responsible for development and implementation of nonclinical strategies for AAV gene therapy products for treatment of rare neurologic disorders. Before joining Sangamo, Jay was responsible for all aspects of safety in product development roles with increasing responsibility at Elanco Animal Health. Jay has a PhD in Pharmacology and Toxicology from the University of Louisville and completed a postdoctoral fellowship at the Medical University of South Carolina.

Sponsors:

UL Research Institutes | Chemical Insights

Department of BIOLOGICAL SCIENCES Clemson University

College of SCIENCE

Erica N. Rogers, Ph.D., DABT
Senior Toxicologist II
Gad Consulting Services

Dr. Erica N. Rogers is a board-certified toxicologist (DABT) with over seventeen years of experience in toxicology, pharmacology, and environmental health sciences. She earned her Ph.D. in Pharmacology and Toxicology from the University of Louisville, where her research examined how curcumin mitigates benzo(a)pyrene diol epoxide (BPDE)-induced DNA damage, followed by postdoctoral research in immunology. Her current work focuses on human health risk assessment and regulatory toxicology, including establishing permissible daily exposure (PDE) limits for pharmaceutical impurities, determining safe exposure levels for extractables and leachables in medical devices (ISO 10993-17), and assessing nitrosamine-related risks. Dr. Rogers has coauthored several publications and book chapters and was recently recognized with an Honorable Mention by the Society of Toxicology's Medical Device and Combination Product Specialty Section. Outside of work, she enjoys mentoring young scientists, leading a Junior Girl Scout troop, and spending time with her family and dog, Bella.

Lauren Wills, Ph.D.
Associate Professor
Charleston Southern University

Dr. Lauren Wills is an Associate Professor of Biology at Charleston Southern University. She teaches courses in General Biology, Environmental Policy and Law, Environmental Toxicology, and the accompanying labs. Dr. Wills earned a PhD in Environmental Science and a certificate in Toxicology from Duke University. After completing her dissertation, she worked as a postdoctoral researcher at the Medical University of South Carolina and as a research specialist for MitoHealth, Inc. As an industry and academic researcher, she developed a high-throughput respirometric assay to measure mitochondrial function and successfully completed multiple high-throughput screens that identified novel mitochondrial toxicants as well as potential therapeutics. Dr. Wills is deeply committed to researching new methods of engaging communities about the intersections between faith, health, and the environment.

Sponsors:

UL Research Institutes | Chemical Insights

Department of BIOLOGICAL SCIENCES Clemson University

College of SCIENCE

Xiaojia He, Ph.D.
Senior Research Scientist
Center for Toxicology and Human Health, Research Institutes' Chemical Insights

Xiaojia He, Ph.D., is a senior research scientist at the Center for Toxicology and Human Health within UL Research Institutes' Chemical Insights. His research focuses on systems toxicology, studying how environmental exposures, such as heavy metals and VOCs, affect host-microbiome interactions and human health. Using multi-omics approaches, he aims to identify biomarkers that bridge critical gaps in the exposure-to-disease continuum, ultimately helping mitigate health risks. Dr. He earned his Ph.D. from the University of Georgia in microbial bioenergetics and redox dynamics, followed by a postdoctoral fellowship at Emory University on heavy metal impacts on the gut microbiome and lung health. He has received multiple honors, including the Annual Award for Outstanding Research Achievement, Dissertation Completion Award, Best Paper of the Year, and Young Investigator Award from various organizations, as well as recognition as one of the World's Top 2% Scientists by Stanford/Elsevier. He has authored 50 peer-reviewed articles with over 3,000 citations, serves as editor and reviewer for multiple journals, and contributes as a conference organizer and session chair.

Kylie Rock, Ph.D.
Assistant Professor
Clemson University

Dr. Kylie Rock is an environmental and reproductive toxicologist whose research bridges human health and ecology to understand how pollutants affect fertility, development, and ecosystem function. She leads the Repro-Eco Tox Lab at Clemson University, where her team investigates environmental contaminants, including endocrine-disrupting chemicals such as PFAS and phthalates, as well as pollutants like mercury and microplastics, using approaches that span molecular to ecosystem scales. Dr. Rock earned her Ph.D. in Toxicology from North Carolina State University and completed postdoctoral fellowships at the University of Maryland School of Medicine and North Carolina State University. Her work has been recognized for both translational impact and community engagement, including the Clemson University College of Science Excellence in Community Outreach Award (2025) and NIEHS Extramural Paper of the Month (2023, 2018). In addition to her academic role, she serves as President of the Southeastern Regional Chapter of the Society of Toxicology and Junior Councilor for the Reproductive and Developmental Toxicology Specialty Section, where she is committed to mentoring the next generation of toxicologists.

Sponsors:

UL Research Institutes | Chemical Insights

Department of BIOLOGICAL SCIENCES Clemson University

College of SCIENCE

Postdoctoral Platform Session

Carbon Black particles induce emphysema and inflammasome activation: a whole-mouse lung proteome landscape

Nilda Sanchez, Ph.D.
University of Alabama at Birmingham

Background and purpose: Chronic exposure to ultrafine particles (UFP) for is one of the leading causes of morbidity and mortality worldwide. The accumulation of UFP is cleared by engulfment of these particles by alveolar macrophages (AMs). AMs are the first line of defense against pathogens, as well as also have anti-inflammatory function for the resolution of the inflammation. The effect of nCB exposures on the anti-inflammatory functions of macrophages are not explored in detail. We are exploring the effects of nCB on the anti-inflammatory function of AMs; efferocytosis, for the homeostasis, and resolution of inflammation. In our preliminary studies, we have developed a mouse model of chronic nCB exposures, and its effect on the lung morphology and injury. We have performed the proteomics analysis to identify the dysfunctions, and mechanisms caused by nCB exposures. **Methods:** C57BL/6 mice (n=5) were exposure to 2 doses of nCB (by oropharyngeal aspiration) each other day during one week. Nanosized Carbon Black (nCB) (15 to 75 nm) was utilize to perform these exposures. After treatment, all mice were euthanized and lungs were harvested for histopathology and whole-proteomic using mass spectrometry LC/MS. All animal protocols were approved by Institucional Animal Care and Use Committee at the University of Alabama at Birmingham (UAB). **Results:** *In vivo* study showed 1) increased inflammation by increased presence of lymphocytes in the lung, 2) alveolar macrophages full of engulfed nCBs, 3) increase alveolar space (emphysema) in the nCB lungs, and increased cell death. Our preliminary proteomic data identified 1894 total proteins across samples. We found 181 significant differential expressed proteins in lung proteome exposed to nCB particles. The histology, and proteomic analysis both demonstrated emphysema, and increased cell death related pathways. The functional enrichment analysis showed that nCB top differential expressed proteins are involved in inflammasome activation, reduction of vesicle trafficking, endosome formation, and calcium signaling process. This proteomics analysis showed nCB differential expressed proteins are associated with emphysema development such as cell death, dysregulation of ubiquitination and ROBO signaling pathways. **Conclusion:** UFP lung exposures induced a differential protein expression pattern showing there's saturation of macrophages capacity to clear nanoparticles and tissue damage**.** Inflammasome activation and suppression of endosomal and lysosomal related proteins suggested an exhaustive of lung macrophages function after nCB exposure. After these studies, we will perform in depth, studies for determining the role of nCB exposures in the development of COPD and emphysema.

Graduate Student Platform Session

Masters

Disruption of Energy Homeostasis by Chemical Mixtures Containing Persistent Pollutants in HepG2 and C2C12 Cells

Morgan Jacobellis

Clemson University

Background: Metabolic disruption and obesity are ongoing public health problems linked to chemical exposure. However, understanding causal pathways is difficult as real-world exposures occur as complex chemical mixtures rather than single chemicals. To improve understanding of the toxic effects of chemical mixtures, we obtained a set of real-world exposure mixture profiles derived from chemical biomonitoring data collected from the Environmental Influences on Child Health Outcomes Fetal Growth Studies (ECHO-FGS) birth cohort. The mixture profiles characterized five distinct exposure scenarios that consisted of varying observed concentrations of p,p'-DDE, PCB153, BDE47, and PFOS. While nuclear receptor signaling has been linked to metabolic dysregulation, mitochondria may also be a direct target of chemical exposure. These mixtures were evaluated for their effects on mitochondrial metabolism in two cell lines. The purpose of this work is to elucidate a mechanism how in utero exposure to mixtures of persistent pollutants may correlate to perturbed weight from birth through childhood. **Methods:** Observed concentrations of chemical mixture profiles of p,p'-DDE, PCB153, BDE47, and PFOS were examined at 1X, 50X, 250X, or 500X. Mixture profiles consisting of the four chemicals were tested individually, in chemical combinations, and as complete mixtures. We tested for mixture effects on metabolic disruption by examining whether the individual chemicals, chemical combinations or chemical mixtures perturb mitochondrial metabolism. Mitochondrial metabolism was measured as Oxygen Consumption Rate (OCR) after 1-hour or 24-hour exposures in HepG2 human hepatocarcinoma or C2C12 murine myoblast cells using MitoStress Tests on an Agilent Seahorse XFe24 Analyzer (Agilent Technologies, Santa Clara, CA). **Results**: MitoStress assays performed in HepG2 and C2C12 cells revealed that mixture Profiles 1, 3 and 4 perturb mitochondrial metabolism. Profile 3, dominated by BDE47, increased Basal Respiration, ATP-Coupled Respiration, Proton Leak, and Maximal Respiration greater than profiles 1 and 4 that are dominated by p,p'-DDE and PFOS, respectively. Interestingly, C2C12 cells were most sensitive to mixture exposures after only 1 hour; HepG2 cells were more sensitive after 24 hours. This suggests different mechanisms of action and a mechanism that is not dependent on transcriptional changes in C2C12 cells. PPAR activation has been hypothesized as a possible mode of obesogenic action; however, this is unlikely in C2C12 cells. Different combinations of chemicals were tested to determine the chemicals that might interact with BDE47. Chemical combinations revealed BDE47 negatively interacted with p,p'-DDE and PFOS. However, the dominant chemical typically drives the predominant effects measured on the mitochondria across profiles. Effects on the mitochondria were observed in multiple cell types and timepoints with greater sensitivity in C2C12 cells at serum-equivalent concentrations (1X) measured in mothers, indicating mitochondrial sensitivity. **Conclusions:** These findings highlight mitochondria as a potentially sensitive target of persistent organic pollutant mixtures. These mixtures perturbed mitochondrial metabolism in multiple cell types, concentrations and time points. Maternal serum equivalent concentrations produce significant short-term mitochondrial effects, highlighting the relevance of these exposures. Together, these results suggest that perturbation of mitochondrial function may be a mechanistic link between exposure to mixtures of persistent organic pollutants and metabolic dysregulation, potentially relevant to child health outcomes.

Doctoral

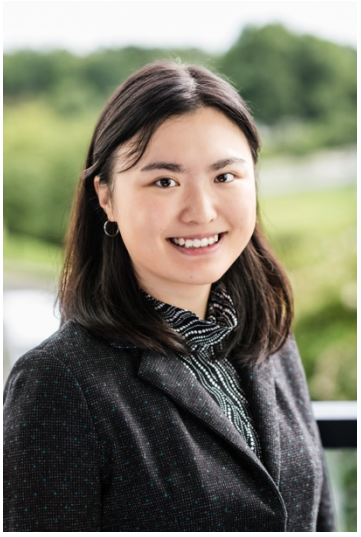

A Comprehensive Database and Harmonization Framework for Standardizing Nanoparticle Biodistribution Studies

Xinyue Chen
University of Florida

Background and Purpose: Nanoparticle-based drug delivery systems represent a rapidly expanding field in nanomedicine, yet the lack of standardized reporting units across biodistribution studies severely limits meta-analyses and computational modeling efforts. Literature reports utilize inconsistent units (%ID, %ID/g, μg/g, nmol/g, mg/mL) and dosing metrics, creating significant barriers for cross-study comparisons and systematic reviews. This study presents the development of a comprehensive Nano-Drug Database with an integrated data harmonization workflow to address these critical standardization challenges. **Methods**: We developed a systematic classification framework categorizing nanoparticles into three distinct types: Type A (therapeutic nanoparticles where NP itself is the active agent), Type B (drug-loaded carriers with encapsulated/entrapped drugs), and Type C (covalently bound drug systems). A comprehensive Standard Operating Procedure (SOP) was established featuring universal conversion equations for biodistribution data standardization. Target units include %ID, %ID/g, and μg/g tissue for therapeutic threshold analysis. The workflow incorporates type-specific conversion protocols accounting for drug loading rates, encapsulation efficiency, drug-to-carrier ratios, and conjugation efficiency. For dose standardization, we implemented equations enabling bidirectional conversion between nanoparticle and drug doses using molecular mass calculations, drug loading calculations (for Types B and C), and comprehensive dose conversion protocols. Default physiological parameters were established including standardized mouse body weight, organ weight fractions, and drug loading parameters when unreported in original studies. **Results**: The harmonization framework successfully processes biodistribution data across all three nanoparticle categories, enabling conversion between concentration units and standardization of administration doses to mg/kg mouse body weight. Preliminary database analysis encompassed 297 studies spanning 2005-2021, revealing significant heterogeneity in reporting practices. The SOP addresses four distinct data reporting scenarios: total nanoparticle concentration, separate drug concentration, combined reporting, and single component concentration. Type-specific protocols demonstrated successful conversion of complex drug-carrier systems, with Type B systems requiring encapsulation efficiency and drug loading parameters, while Type C systems necessitated drug-to-NP ratios and conjugation efficiency data. The framework accommodates studies reporting only radioactive doses through specific conversion protocols utilizing specific activity measurements. **Conclusions:** The Nano-Drug Database systematically harmonizes nanoparticle and drug biodistribution data across diverse reporting formats and nanoparticle types. This standardization framework enables robust meta-analyses, computational modeling, and cross-study comparisons previously impossible due to unit inconsistencies. The type-specific classification system provides a foundation for evidence-based nanomedicine development and regulatory assessment. Future applications include physiologically based pharmacokinetic (PBPK) and machine learning model development for biodistribution prediction and systematic evaluation of nanoparticle design parameters affecting therapeutic efficacy. This work establishes critical infrastructure for advancing nanomedicine through data-driven approaches and predictive modeling capabilities essential for rational nanoparticle design and clinical translation.

Perfluorohexane sulfonate (PFHxS) induced developmental toxicity is susceptible to photoperiod perturbations

Syed Ferdous
Clemson University

Background & Purpose: Light is a primary environmental cue that shapes the biology of nearly all organisms. In vertebrates, rhythmicity is regulated by molecular feedback loops involving circadian clock genes, coordinated to external light via retinal photoreceptors and the suprachiasmatic nucleus (SCN). These 24-hour rhythms, generated by transcriptional–translational loops in nearly all cells, control essential processes such as metabolism, hormone secretion, redox balance, DNA repair, and xenobiotic detoxification. Considering these aspects, seasonal variations in photoperiods as well as artificial exposure to light from electronic devices and shift work can modify toxicity of xenobiotics that act through similar mechanisms. However light and photoperiod as a variable factor in toxicology is often overlooked. This omission is especially critical for persistent contaminants such as perfluoroalkyl substances (PFAS). Among PFAS, perfluorohexane sulfonate (PFHxS) has emerged as a key toxicant due to its persistence in ecosystems. Its strong carbon–fluorine bonds confer thermal and biological stability, leading to widespread detection. PFHxS exposure has been linked to metabolic and neurological adverse effects- processes that are known to be regulated by the circadian system. Our prior larval photomotor response (LPR) data showed that PFHxS shows photoperiod-dependent behavioral patterns, reinforcing the need to examine light as a determinant of developmental toxicity. This study addresses the knowledge gap in understanding photoperiod-PFAS interactions and examines how photoperiod variations modify PFHxS developmental toxicity by integrating transcriptomic and molecular readouts. **Methods:** Embryos were exposed to 0, 0.0025, or 25 µM PFHxS from 2–120 hpf under 14L:10D (14 hr light: 10 hr dark) or 24D (24 hr dark) photoperiod conditions. LC-MS was conducted to analyze PFHxS uptake and mRNA sequencing was conducted on an Illumina platform. Transcription factor–gene interactions were inferred using g:Profiler, TFmiR3, and Cytoscape, with hub networks identified via cytoHubba. For assessment of reactive oxygen species (ROS), embryos were stained with H_2DCFDA, and imaged with a fluorescence microscope. DNA damage was assessed by phospho-H2AX whole mount immunohistochemistry. For assessing cell proliferation, embryos were pulsed with BrdU and stained with anti-BrdU antibody before imaging and categorical scoring. **Results:** LC-MS data showed equivalent embryo-wide PFHxS uptake under both photoperiods. At 25 µM, PFHxS exposures resulted in 578 and 2912 differentially expressed genes under 14L:10D and 24D conditions respectively, indicating that the response was stronger under 24D. KEGG pathway analysis revealed that several pathways were commonly affected by PFHxS under both 14L:10D and 24D conditions. This included downregulation of cell cycle, DNA replication, and drug metabolism pathways, along with upregulation of metabolic pathways and neuroactive ligand-receptor interactions. However, 14L:10D uniquely affected pyrimidine metabolism and PPAR signaling, whereas 24D uniquely altered MAPK, autophagy, insulin signaling and base excision repair. Transcription factor (TF) network analysis further highlighted photoperiod specificity. Under 14L:10D, hubs included *MCM2, MYB, UHRF1, E2F8,* and *IGFBP1*, emphasizing developmental and metabolic control. Under 24D, hubs shifted toward stress and repair, including *E2F1, JUN, MCM2, MCM5, and PTTG1*, reflecting damage-responsive regulation. This network configuration reflects a transcriptional emphasis on DNA damage response, redox imbalance, and cell cycle checkpoint activation, indicating that photoperiod disruption reorients PFHxS responses away from developmental and metabolic programs toward pathways that prioritize cellular defense and repair. Since our transcriptomic data led towards stress and DNA repair signaling, we further conducted assays for ROS, DNA damage and cell proliferation. Our ROS assay revealed 26.42% increase under 14L:10D and 49.91% increase under 24D, indicating that photoperiod changes impacts ROS levels. Likewise, for DNA double strand breaks, we saw a 32.4% increase in H2AX staining compared to the DMSO control under 14L: 10D, but a dramatic 80.6% increase under 24D, suggesting a photoperiod-specific effect. We also saw an inhibition of cell proliferation on BrDU staining, but these effects were not susceptible to photoperiod changes. **Conclusion:** Our findings showed that photoperiod is a critical factor in shaping the developmental toxicity of PFHxS. Differences

in photoperiod altered baseline circadian programs and modulated the severity of PFHxS-induced effects on gene expression, oxidative stress, DNA damage, and cell proliferation. Incorporating photoperiod as an experimental variable is therefore essential for understanding chemical toxicity.

Sex-Dependent Alterations in Gut Motility, Short-Chain Fatty Acids and Peripheral Organ Weight Following Gulf War Chemical Exposure: Modulation by Inulin and LNFPIII

Trevor Kalinowski
University of Georgia

Gulf War Illness (GWI) is a chronic multi-symptom illness experienced by 30% of deployed U.S. veterans, 7% of whom were female, linked to a combination of chemical exposures during the 1990-91 Persian Gulf War. Exposures included the overuse of prescribed packs of reversible acetylcholinesterase inhibitor, pyridostigmine bromide (PB) and excessive use of insecticide permethrin (PM). GWI symptoms are chronic and include neurological, as well as gastrointestinal (GI) issues. GI perturbations affect the gut microbiome and GI permeability in GWI models contribute to long-term perturbations of the gut-brain axis (GBA). Short-chain fatty acids (SCFAs) are key byproducts of gut microbes and reflect healthy GBA activity. Here, we examined chronic outcomes of GWI exposure in male and female C57BL/6J mice using gut transit assays, SCFA profiling, organ and tissue weight measurements, with additional evaluation of dietary and immunomodulatory interventions. 8-week-old C57BL/6J mice received PB(0.7mg/kg) and PM (200mg/kg) (PB/PM) intraperitoneally for 10 days and allowed to age with access to food and water *ad libitum*. At 6 months, baseline gut transit was assayed using Carmine red dye, the time of red pellet pass was measured over 6 hours. Prior to this assay, fecal pellets were collected and weighed for SCFA analysis of acetate, propionate, butyrate, valerate, caproate measured by GC–MS. At 8 months, mice underwent dietary manipulation, receiving isocaloric diets containing 1% cellulose or without 2.5% inulin, and received either the immunomodulatory glycan Lacto-N-fucopentaose III (LNFPIII) or vehicle dextran (50µg) twice per week for 1 month, followed by gut transit assay and SCFA analysis. Treatment and diet continued until 12–13 months, where mice were sacrificed for organ and tissue collection (liver, ileum, spleen, subcutaneous (SQ) and retroperitoneal fat (RP), brown adipose tissue (BAT), slow twitch (STM), and fast twitch (FTM) muscles). Weights were normalized to total body weight. At 6 months, GWI females showed a significant shift in SCFAs, specifically reduced acetate: propionate ratios. At 9 months, however, gut transit was impaired by GWI, specifically in males absent inulin. Female gut transit was not significantly perturbed by GWI, but inulin numerically improved gut motility in controls. GWI exposure had a bidirectional effect on acetate and total SCFAs. Thus, significant and trending increases in males, but significant decreases in female control mice absent LNFPIII or inulin, respectively, were observed. Inulin overall, significantly increased propionate and butyrate, in both sexes. This effect, however, was synergistic with LNFPIII treatment in females exclusively which ameliorated GWI effects observed in butyrate levels. Conversely, males absent GWI, displayed a significant increase in butyrate from LNFPIII treatment. At 13 months, GWI exhibited bidirectional effects on ileum weights decreasing and increasing in male and female GWI mice, respectively. This effect was ameliorated in males given LNFPIII with or without inulin. BAT was also decreased in both sexes by GWI overall but ameliorated by LNFPIII and inulin together in females. Male spleen and FTM, exclusively, were reduced by GWI overall, and rescued by LNFPIII and inulin together. Female STM weights mirrored these effects, exclusively. Collectively, PB/PM exposure produces metabolic effects overall, and male-specific effects on gut motility, indicative of prior preclinical models. Lower GI inflammation in veterans is widely reflected in PB/PM models through gut permeability and chronic constipation, respectively. Increased butyrate and propionate levels reflect intestinal energy and potential GBA recovery, respectively. Inulin-fed females, support this via intact gut motility highlighting improved gut metabolic presence overall. Conversely, GWI male ileum weights recovered, but still exhibited compromised gut motility and metabolic mechanisms highlighting complex gut dysbiosis mechanisms of GWI that are male-specific. Inulin and or LNFPIII treatment underscore sex-dependent targeted interventions into amelioration of gut dysbiosis in

GWI veterans as promising efficacious therapeutics. This project was supported by the Department of Defense (W81XWH2110661) and the University of Georgia Interdisciplinary Toxicology Program (ITP). We thank Dr. Norberg for synthesizing and Dr. Harn for validating LNFPIII for this study.

Sponsors:

UL Research Institutes | Chemical Insights

Department of BIOLOGICAL SCIENCES Clemson University

College of SCIENCE

Poster Presentations by Number:

Sorted by degree and alphabetically by last name

Sponsors:

17	Melanie Garcia, *Clemson*	Assessing the effects of p,p'-DDE, PCB153, BDE47, and PFOS mixtures on adipocytic differentiation of 3T3-L1 cells	27
18	Hailey Levi, *Univ. of Alabama at Birmingham*	Low dose exposure to Dihydroxyacetone (DHA) changes to cardiac metabolism and induces DNA damage	28
19	Erin Levon, *Clemson*	Using human-induced pluripotent stem cell derived motor neurons to assess a critical period of susceptibility to sodium arsenite during development	29
20	Xiao Li, *Clemson*	Polyvinyl chloride nanoplastic induces mitochondrial damage in human cardiomyocytes	29
21	Ignacio Llada, *Univ. of Georgia*	Metabolomic shifts in beef steers rotationally grazing toxic endophyte-infected tall fescue under fall conditions	30
22	Carlos Eduardo Bastos Lopes, *Auburn*	Acute Exposure to PEGylated Gold Nanoparticles Cause Mitocondrial Dysfunction: The Role of AuNPs' shape	31
23	Taylor Martin, *Univ. of Georgia*	Novel Function of Emergency Contraceptives in Disrupting Uterine Fluid Dynamics	32
24	Kristofer Meier, *Univ. of Georgia*	Altered ovarian steroidogenesis as a mechanism for the effects of endocrine disrupting compounds on the uterus	32
25	Alyssa Meyers, *Univ. of Florida*	Impact of Developmental Exposure to Environmental Levels of PFAS and PFAS Mixtures on Multi-tissue Transcriptomic Profiles in Adult Zebrafish	33
26	Kanchaka Senarath Pathirajage, *Clemson*	Aryl hydrocarbon receptor (AhR2) Signaling Mediates Tetrabromobisphenol A (TBBPA) Toxicity in Zebrafish	34
27	Paige Powell, *Clemson*	Protecting Predators: A Non-Lethal Framework for Toxicological Risk Assessment in Sharks	34
28	Beverly Thomas, *Auburn*	Polymer-Specific and Time-Dependent Toxicity of Textile-Derived Microfibers in Fish Gill Cells	35
29	Emma Vander Meulen, *Univ. of Florida*	Persistently Distinct PPCP Contaminant Profiles in the Lake Huron–Lake Erie Corridor: A Multi Year NMDS Study	36
Postdoctoral			
30	Chi-Yun Chen, The *Univ. of Florida*	Interpretable machine learning reveals key drivers of inorganic nanoparticle cytotoxicity	38
31	Ho Young Lee, *Emory*	Sex-Dependent Disruption of Adiposity and Vitamin D3 Metabolism by Microbiome-Derived Delta-Valerobetaine in Aged Mice	38
32	Gopikrishnan Mani, *Univ. of Alabama at Birmingham*	Cadmium Promotes Extracellular Mer Generation via ADAM17, Impairing Efferocytosis and Contributing to the Pathogenesis of Emphysema	39
33	Allie Smith, *Univ. of Alabama at Birmingham*	The effects of trichloroethylene exposure on cognitive behavior in PFF-injected mice.	40

Sponsors:

UL Research Institutes | Chemical Insights

Department of BIOLOGICAL SCIENCES Clemson University

College of SCIENCE

Undergraduate Poster Abstracts

Investigating the Antimicrobial Effects of a Novel Dual Zwitterionic Alkyne
Isabelle Clark
King University
This research aimed to study antimicrobial properties of a dual zwitterionic alkyne (DZA), a novel molecule synthesized previously by members of our research group. DZA is a symmetric molecule consisting of a sulfobetaine group on each side of the central alkyne. The sulfobetaine groups each contain both a quaternary amine and a sulfonate group. Quaternary amines often show antimicrobial activity by binding to negatively charged bacterial membranes and disrupting their growth. The focus of this research is to test whether this novel DZA compound has antimicrobial effects. Prior studies indicate that antimicrobial activity of similar zwitterionic compounds can vary based on carbon chain length. As this is a relatively new molecule, exploring its fundamental biological and chemical properties will allow for a wider array of uses for this compound. Preliminary research suggests that relatively high concentrations of the DZA solution did little to no harm to *Caenorhabditis elegans*. This research tested DZA against Gram-positive and Gram-negative bacteria using a disk diffusion assay to determine antimicrobial activity. Initial testing has indicated that the DZA molecule does not inhibit growth of *Escherichia coli* or *Staphylococcus aureus.* Further studies will help identify other potential antimicrobial properties of the DZA molecule, opening opportunities for further research on its possible uses in commercial applications.

PFAS Concentrations and their Effect on Microbial Communities in Urbanized and Non-urbanized South Carolina Estuaries
Romina Dotson
Clemson University
An estuary is an aquatic biome that plays a significant role as a nursery to many organisms, regulating biological cycles, and being a transition zone of freshwater and saltwater. Estuaries are essential to many ecosystems due to these properties but have been heavily affected by the growth of coastal urbanization. One impact of urbanization is the contamination of nearby water systems with chemical pollutants. A class of pollutants of significant concern are per- and polyfluoroalkyl substances (PFAS), which have been detected in waters and sediments worldwide. In estuaries located on coastal South Carolina, high PFAS concentrations have been detected in urbanized estuaries such as Charleston Harbor. As urban estuaries continue to be polluted with PFAS, more data needs to be collected to understand the impact of PFAS on these ecosystems, including the microbial communities that regulate biogeochemical and nutrient cycling. One of many functions that microbial communities perform is pollutant degradation, which could be helpful to estuaries affected by high PFAS concentrations. Despite disruptions to microbial communities and abundance caused by PFAS, resistant microbes continue to persist in estuarine systems. The objective of this study is to compare PFAS concentrations and microbial community composition in two South Carolina estuaries that differ in urbanization: Charleston Harbor (CH, urbanized) and St. Helena Sound (SHS, less urbanized). We hypothesize 1) PFAS concentrations in surface water and sediment samples from CH will be higher than in SHS; and 2) higher PFAS concentrations will lead to increased abundance of PFAS resistant microbes that have the potential to degrade PFAS. We used high-performance liquid chromatography tandem mass-spectrometry (HPLC-MS/MS) to quantify PFAS concentrations from sediment and water samples collected in October 2024, and January of 2025. To characterize microbial communities, 16S rRNA sequencing was employed to assess alpha, beta, and taxonomic diversity for each site and month. Pipette analysis will also be performed to reveal the type of sediment particles located at all sites. Our preliminary data revealed that PFOS concentrations were greater in SHS than CH. The sediment analysis revealed that the type of sediment present in estuaries had no correlation to PFAS concentrations. The diversity analysis showed there are distinct differences in microbial communities at both sites, and across seasons. However, these trends may not be linked to PFAS as multiple factors play a role in microbial makeup. Ongoing studies include performing controlled microbial exposures by culturing sediment

bacteria under aerobic and anaerobic conditions. We aim to evaluate microbial response to PFAS exposure and identify bacterial species with potential to degrade PFAS. With these results we could provide information on how microbes could be used in bioremediation efforts and the role they play in estuary ecosystem health.

Investigating protective effects of nicotine on pesticide induced dopaminergic neurodegeneration in *C. elegans*

Cassie Lane
King university

Parkinson's Disease (PD) is the second most prevalent neurodegenerative disease, characterized by tremors, bradykinesia, and impaired coordination and balance. PD results from the degeneration of the dopaminergic (DA) neurons in the substantia nigra, a critical region of the brain involved in movement control. The etiology of PD is multifactorial but is understood to be an interaction of genes and the environment, especially pesticide and heavy metal exposure. There is no cure for PD, and the few available treatments lose efficacy over time; therefore, there is a need to understand the mechanisms leading to PD. Mancozeb, a common fungicide, contains the active ingredient manzate or Mn/Zn ethylene-bis-dithiocarbamate, and is known to disrupt neurotransmission and increase oxidative stress. Previous research in our lab has indicated that the fungicide Mancozeb induces PD, like dopaminergic (DAergic) degeneration in the model organism *C. elegans* by inhibiting complex I of the mitochondrial electron transport chain. In humans, epidemiological studies have shown that PD is less frequent in nicotine users, although the protective effect and potential mechanism are unknown. Nicotine has a high binding affinity to the nAChRs (nicotinic Acetyl-Choline Receptors) in DAergic neurons and has been shown to modulate DAergic signaling, reduce oxidative stress, and improve mitochondrial function. It is proposed that this binding may lead to a protective effect. To investigate the role of nicotine in pesticide-induced DAergic degeneration, wild type *C. elegans* (N2) and a fluorescently tagged strain (BY250) were treated with either nicotine or manzate individually, a dual treatment of nicotine followed by manzate, and a control of no treatment. DAergic neuron function was monitored by two behavior-based assays. A mechanosensation assay was performed, with the nose touch assay targeting DAergic neurons, soft touch targeting Touch Receptor Neurons (TRNs), and harsh touch serving as a general response control. The DAergic system also controls movement and feeding behavior. The basal slowing response was observed to monitor their locomotion with and without the presence of a food source (E.coli). Taken together, the combination of these assays provides important insight into the potential protective effect of nicotine on pesticide-induced DAergic neuron degeneration, leading to a better understanding of how nicotine may decrease the risk of developing PD and open potential avenues for understanding underlying mechanisms and finding new treatments.

Culturing Primary Human Cytotrophoblast Cells to Investigate Xenobiotic Transporters at the Blood-Placenta Barrier

Alexandra Suggs
Clemson University

A majority of people who are pregnant use at least one medication during pregnancy; However, most drugs are administered off-label lacking much needed information about the dose, maternal fetal pharmacokinetics, safety, or efficacy. Major concern has been raised regarding how these drugs are transferred across the placental barrier and what effects they may have on the exposed fetus. The placenta is a barrier that serves to control the flow of maternal nutrients to the fetus. As a maternal- fetal organ, placental cells express both maternal and fetal genetic material, including the fetal sex chromosomes XX or XY. We hypothesize that sex differences in teratogenicity of xenobiotics is, in part, dictated by sex specific expression and/or activity of xenobiotic transporters within the placenta leading to discrepancies in exposure for male and female fetuses. Through our partnership with the OBGYN department of Prisma Health, I collected biopsies from human placental samples delivered via cesarean section. Samples were 1) frozen and extracted for rna to analyze the expression of 15 major drug transporters or 2) placed in phosphate buffered saline and kept on ice. To isolate and culture primary cytotrophoblast cells I used quantitative real-time PCR (qRT-PCR) to assess mRNA expression in 3 male and 3 female placenta samples, however, no significant difference in gene expression

was observed. Using immunohistochemistry I was able to observe the differentiation of cytotrophoblast cells into multinucleated syncytiotrophoblasts in culture. We are currently working on analyzing additional samples to increase our sample size for qRT-PCR and more consistent results, and ultimately provide insights into how sex plays a role in the expression and activity of xenobiotic transporters at the blood-placenta barrier, utilizing eFLUXX assays to probe for the sex-specific differences in transporter activity. Forward future steps include continuing to collect and analyze placenta samples, carrying out the various procedures above eventually for a larger sample size. Collectively, this work will advance the field's knowledge about biological factors that may contribute to differences in male and female vulnerability to xenobiotics *in utero.*

Microplastics in Macroinvertebrates: An Analysis of Microplastics in Freshwater Ecosystems in Upstate South Carolina

Sophie Waugh
Clemson University

Microplastic (MP) pollution is a growing environmental, ecological, and public health threat globally. The exponential increase in production and demand of plastic since the 1950s has called for an increase in attention to the widespread and rising threat of MP accumulation in the environment. Despite its growing importance, much remains unknown about the abundance, distribution, and spread of MPs in a given watershed. Previous research on MPs has concentrated on marine environments, often overlooking their presence and impact in freshwater ecosystems. To assess MP presence in freshwater, we first examined MP quantity and type in the sediment of two streams near Clemson, SC: Hunnicutt Creek (HC), bordered by high-intensity development, and Eighteenmile Creek (EM), bordered by low-intensity development. We also assessed MP loading in benthic macroinvertebrates, as MPs can be ingested by freshwater organisms. Upon field collection of samples, a combination of wet peroxide oxidation and density separation methods were used prior to visual inspection under a microscope. MPs were positively identified using the hot needle test, then counted and categorized by type and color. We hypothesize that the predominant type and color of MPs will be consistent between sediment and macroinvertebrate samples, suggesting that macroinvertebrates ingest MPs present in the sediment. We further hypothesize that MP concentrations will be higher in HC samples than in EM, reflecting HC's closer proximity to areas of high-intensity development. Preliminary results from the spring of 2025 showed that 18 MPs were recovered from 89 organisms collected from EM, and in HC, a total of 23 MPs were recovered from 32 organisms. Six sediment cores from HC and four sediment cores from EM were also processed. Average MP sediment loading in EM was 0.041 ± 0.009 particles g^{-1} and 0.047 ± 0.01 particles g^{-1} in HC. In both sediment and macroinvertebrate samples, clear fibers were the most abundant MP identified. While these early findings suggest higher MP presence in HC relative to EM, additional samples and data collection are ongoing. The results from this study will serve as an indicator of MP contamination in freshwater biota and their environment in the Upstate of South Carolina. Ultimately, these findings will provide a foundation for further investigation in under-researched regions of the Southeast and encourage research efforts focused on solutions to MP pollution in natural systems.

Master's Poster Abstracts

Early developmental toxicity of polycyclic aromatic hydrocarbons (PAHs) phenanthrene and fluoranthene: cytoskeleton as a target

Alfredo Rojas
Clemson University

Background and Purpose: Polycyclic aromatic hydrocarbons (PAHs) are a class of organic compounds that are typically produced by incomplete combustion. Members of the PAH family can be further divided into low molecular weight and high molecular weight by the number of rings they contain. Higher ring PAHs have been shown to have higher toxicity than their lower ring counterparts. PAHs are known to be detoxified through aryl hydrocarbon receptor (AHR) activation, resulting in increased levels of detoxification genes such as *cyp1a*. While much has been studied about the long-term effects of PAHs and their developmental toxicity through the AHR pathway, few studies have gone in depth on how they impact early developmental processes, when the embryonic architecture begins to take shape. Using zebrafish as a model organism, our study investigates the impacts two widely occurring PAHs- fluoranthene and phenanthrene- during the pre-pluripotent stages of embryogenesis. **Methods**: PAH concentrations were quantified via UV-fluorescence spectrophotometry. Following plating and PAH exposure, solutions were collected, and fluorescence was estimated at 2, 4, and 6 h post fertilization (hpf) at an excitation/emission of 358nm/466nm for fluoranthene and 275nm/367nm for phenanthrene. For phenotyping, embryos were exposed to 0, 6.25, 12.5, 25, 50, and 100 µM concentrations of both phenanthrene and fluoranthene at 0.75hpf (~2-4 cell stage), followed by assessments of mortality at multiple developmental stages. To understand the genetic underpinnings of observed effects, mRNA-seq was conducted on embryos exposed to 0 or 100 µM of phenanthrene or fluoranthene on an Illumina platform, with bioinformatics analyses conducted using DeSeq2. To assess the role of the cytoskeleton, embryos were exposed to 0 or 100 µM of phenanthrene and fluoranthene, followed by staining with Alexa Fluor 488-conjugated phalloidin probe (for F-actin) or immunostaining with α or β tubulin. To examine reactive oxygen species (ROS), embryos were exposed to PAHs at 0.75 to 3.5hpf and stained with an ROS stain (CH2-DCFH-DA). To examine if co-exposure to N-acetylcysteine (NAC), an antioxidant, rescues PAH-induced phenotypes, embryos were exposed 0 or 100 µM PAH in presence of absence of 100 µM NAC, followed by developmental phenotyping, cytoskeletal staining, and ROS quantification. All images were taken on an Echo Revolve Microscope, either in brightfield or FITC filter. Fluorescence and morphometric quantifications were conducted within Image J, using 1 or 2-way ANOVA, followed by Dunnett's or Tukey's posthoc tests ($p<0.05$). **Results**: UV-fluorescence spectroscopy revealed a gradual decrease in nominal fluorescence over the first 6 hours of exposure for both PAHs both in the presence or absence of embryos. Embryonic phenotyping showed that both fluoranthene and phenanthrene exposures led to concentration-dependent increases in mortality starting at 4hpf, with 100% mortality in 100 µM exposure by 6hpf. Surprisingly, mRNA sequencing data did not reveal large scale transcriptomic disruptions, with only 4 genes disrupted in the two PAHs. Furthermore, mRNA-seq data, combined with follow-up qPCR and immunohistochemistry, did not reveal any differential levels of *cyp1a* mRNA or protein- a common biomarker for PAHs- suggesting that at these stages, toxicity is AHR2 independent. Assessments of cytoskeletal proteins revealed substantial cytoskeleton disruption, with ~38% and ~30% higher levels of F-actin in the yolk sac, and ~14% and ~13% lower levels in the cell mass for phenanthrene and fluoranthene respectively. Both PAHs also significantly induced ROS at 100µM. Co-exposure with NAC revealed that ROS levels were rescued in phenanthrene treated embryos only. Upon examining the effect of NAC on the cytoskeletal network, there were no large-scale recovery to cytoskeletal damage when co-exposed with PAHs and NAC, indicating that the cytoskeletal disruptions were not related to oxidative stress. **Conclusions**: Our work revealed that both PAHs lead to early developmental mortality that is independent of AHR2-activation. Interestingly, both PAHs induced ROS and disrupted actin patterns, indicating that the impacts of PAH may be driven by ROS-induced cytoskeletal disruptions- a well-studied toxicological phenomenon. However, while ROS induction was rescued by NAC, cytoskeletal patterns were not, suggesting that cytoskeletal damage is not driven by ROS.

Tetrabromobisphenol S (TBBPS) delays embryogenesis and disrupts F-actin expression during zebrafish gastrulation

Rosemaria Serradimigni
Clemson University

Tetrabromobisphenol S (TBBPS) is a new brominated flame retardant (BFR) that serves as an alternative to tetrabromobisphenol A. Previous research has revealed that TBBPS can readily accumulate in environmental matrices and potentially pose risk to environmental and human health. However, being an emerging BFR, there is limited knowledge of its toxic effects. The objective of this study is to use zebrafish as a model and determine the effects of TBBPS exposure on early embryogenesis, encompassing gastrulation – a stage of development when cell fate decisions are made. We initiated TBBPS exposures (0 or 40 μM) at 0.75 hours post fertilization (hpf) and phenotyped their progression hourly through cleavage, blastula and gastrula stages (till ~8 hpf). Our data revealed that TBBPS-treated embryos show delay in development starting at ~5.5 hpf (50% epiboly)- a stage constituting mid-gastrulation, with significant mortality late-gastrulation. To examine the genetic basis of TBBPS-induced effects, we conducted mRNA sequencing on exposures from 0.75 to 7 hpf. Gene ontology and transcription factor analyses revealed downregulation of cytoskeletal organization and tight junctions as a potential pathway for TBBPS-induced developmental delay, processes that are crucial for proper gastrulation progression. To validate these outcomes, we stained for a series of cytoskeletal and tight junction proteins. Among cytoskeletal proteins, F-actin expression was consistently upregulated when exposed to a wide range of TBBPS concentrations (0.004 - 40 μM). Interestingly, our mRNA-seq data showed a ~4.7 fold overexpression of mapk14, a gene that encodes p38 protein- a key regulator of actin. To determine if p38 plays a role in TBBPS-induced F-actin disruption, we co-exposed TBBPS (0 or 40 μM) with a known p38 inhibitor (5 μM SB 203580) and assessed developmental phenotypes and F-actin levels. We revealed a significant recovery in both developmental delay and phalloidin expression, with co-exposure groups exhibiting cell-stages and phalloidin expression similar to controls. Collectively, our genetic and phenotypic data shows that embryonic physiology is vulnerable to early TBBPS exposure, with developmental delays and genetic disruptions during gastrulation stages. We further demonstrate that these effects may be driven by cytoskeletal proteins with MAPK signaling as a mechanistic driver of effects. Ongoing studies are aimed at detailed assessments of the mechanism underlying TBBPS-p38 interactions.

Subtoxic Exposure to "Real-World" Micro/Nanoplastics Triggers Cytosolic ROS and Mitochondrial Remodeling Without Inflammatory Activation in Human Microglia

Seth Vogt
Auburn University

The use of plastic in commercial products has grown exponentially since the material's introduction in the early 1900s. Subsequently, plastics have become a constant in nearly every industry and product on the planet. Recently, micro- and nanoplastics (MNPs) that originate from consumer products (secondary micro/nanoplastics) have recently been identified as contaminants for humans and the environment. Recent studies have been able to identify MNPs in numerous human tissues, including the brain. However, very little is known about the potential health effects caused by these particulates. Currently, most studies involving MNPs rely on "pristine" nanoparticles (NPs), which are mass manufactured to be within certain size and shape tolerances. The impact of "real-world" MNPs, or plastic particulates that would be more relevant to everyday human exposure, still remains largely unexplored. The release of cup- and fork-MNPs is driven by their thermolability and the composition of the material. In this study, we aimed to investigate the cellular impacts of "real-world" MNPs derived from everyday consumer cups and forks (cup-MNPs and fork-MNPs, respectively) on human microglial clone cells (HMC3, brain macrophages). The effects of "real-world" MNPS were complemented with pristine polystyrene nanospheres (PS-50), which up until this point have been a standardized model used in MNP studies. In our experimental design, HMC3 cells were exposed to MNPs at 0.1, 1, and 10 μg/mL for up to 72 hours. MNP characterization was performed using FTIR, which confirmed that the cup- and fork-MNPs were synonymous with spectra of polystyrene. Additionally, ICP-OES analysis of the "real-world" MNPs showed a lack of Pb, Cd, Cr, Ba, Zn, Cu, Ni, or Ag contamination, some of the most common polymer additives and

metals used in polymer synthesis. This allows our research to focus on the impact of particle size and shape rather than chemical composition. MNP and PS-50 exposure up to 72 hours did not yield significant cytotoxicity at any concentration tested. Experimental focus was shifted to the 72- hour timepoint as a trend in the increase in cell viability was found at this timepoint. Concentrations of 0.1 and 1 µg/mL were chosen as the main focus as previous literature reviews determined the concentrations in the human body to be in this range. Cellular ROS were found at elevated concentrations following cell exposure to cup- and fork-MNPs and PS-50 whereas mitochondrial ROS remained unchanged, suggesting an extramitochondrial source of cellular stress. Cells were found to counteract this ROS production with a significant increase in superoxide dismutase 1 (SOD1) activity and an increase in glutathione antioxidant activity. Despite a lack of mitochondrial ROS, results indicated mitochondrial remodeling as significant decreases in mitochondrial mass at MNP concentrations of 1 µg/mL and colocalization with lysosomes were observed, suggesting the occurrence of mitophagy. Cells exposed to 0.1 µg/mL of PS-50 NPs were found to produce significantly less ATP with a corresponding increase in mitochondrial mass, showing the cellular response to lower energy production. This trend was absent in all 1.0 µg/mL samples exposed to cells, where ATP production was not significantly different despite decreased mitochondrial mass. “Real-world” MNPs and PS-50 were found to not induce inflammation as inflammatory biomarkers IL-6, IL- 8, and TNF-a were found to be at nonsignificant concentrations at 0.1 and 1.0 µg/mL exposures. Together, our results indicate a subtoxic exposure to “real-world”, secondary MNPs as well as PS-50 “pristine” NPs can lead to intracellular oxidative stress and an antioxidant response elicited by the cell. Cellular ATP concentrations remaining consistent to control despite a decrease in mitochondrial mass indicates further stress on the cell’s metabolism. It could be concluded that the effects of MNPs and PS-50 at 0.1 and 1.0 µg/mL on human brain cells at subtoxic concentrations interferes with cellular homeostasis but does not result in significant impairment of viability or function.

Drivers of Contaminant Load in Elasmobranchs: Coastal Development and Feeding Ecology

Melissa Walker
Clemson University

Background and Purpose: Pollution is a key driver of biodiversity loss in marine ecosystems and poses risks to sharks, a subgroup of elasmobranchs, as apex predators and keystone species vulnerable to the bioaccumulation of persistent contaminants. Coastal estuaries serve as critical feeding and nursery habitats for many shark species, often overlapping with urban development and pollutant inputs. Although contaminant bioaccumulation varies by species, age class, and trophic position, few studies have examined contributions of coastal urbanization and feeding strategy on elasmobranch body burdens. This research aims to (1) evaluate how residence in urbanized versus non-urbanized estuaries influences contaminant concentrations in broadnose sevengill sharks (Notorynchus cepedianus), and (2) assess how specialist versus generalist feeding strategy affects contaminant levels in finetooth (Carcharhinus isodon) and sandbar (Carcharhinus plumbeus) sharks. I hypothesize that sharks from urbanized estuaries will have higher contaminant concentrations than those from less-impacted areas, and that generalist feeders will accumulate more contaminants due to consumption of higher-trophic-level prey. **Methods**: To test these hypotheses, environmental samples of water and sediment were collected along with shark muscle tissue and blood samples using catch-and-release methods. Project 1 focused on broadnose sevengill sharks from San Francisco Bay, CA (SFB), a highly urbanized estuary, and Willapa Bay, WA (WB), a relatively pristine estuary. Project 2 targeted finetooth and sandbar sharks from Bulls Bay (BB) and St. Helena Sound (SHS), SC, with additional muscle tissue collected from prey species. Structural data (sex, precaudal length, fork length, stretch total length, and estimated age class) were recorded to assess physiological and ontogenetic differences. Project 1 samples also included clasper calcification on males to determine sexual maturity and approximate weight in kg when conditions permitted. Mercury concentrations are quantified via thermal decomposition, amalgamation, and atomic absorption spectrophotometry, while a targeted list of 21 per- and polyfluoroalkyl substances (PFAS) will be analyzed using liquid chromatography–mass spectrometry (LC-MS). Stable isotope (SI) analysis ($\delta^{13}C$ and $\delta^{15}N$), plus prey sample mercury analysis, will further support trophic positioning and contaminant transfer assessment. **Results**: Preliminary Project 1 results show significant differences in muscle total mercury (THg) levels by age class in SFB broadnose sevengill sharks

samples, with subadults having the highest concentrations versus juveniles and neonates/YOY (Young of the Year). Additionally, blood from WB broadnose sevengill shark samples show significant differences in THg between adults and subadults. Across sites, subadult broadnose sevengill shark blood show significantly higher THg levels in samples collected from SFB versus WB. Blood, tissue, water and sediment THg and PFAS analyses are ongoing. In Project 2, blood THg levels in sandbar sharks are significantly higher than those in finetooth sharks by age class, and both finetooth and sandbar THg concentrations trend upward with size, with adults showing significantly higher THg levels compared to younger age classes. There were no significant differences between finetooth neonates/YOY and juveniles/subadults, nor were there differences by sex per age class for both species. Finally, PFAS were detected in water and sediment samples, showing significant differences between BB and SHS for water but not for sediment. Prey, blood, tissue, water and sediment THg, PFAS and SI analyses are ongoing. **Conclusions**: These studies provide insight into how habitat use and ecological traits shape contaminant exposure in elasmobranchs. Findings may support conservation strategies, improve understanding of food web contaminant transfer, and inform risk assessments for vulnerable marine species. **Disclosure**: Project 1 is supported by Save Our Seas Founding (SOSF) grant number 669 awarded to Kylie D Rock. Project 2 is supported by grants funds from the Lerner-Gray Fund for Marine Research of the American Museum of Natural History awarded to Mel Walker. Both projects are additionally supported by Clemson University, Department of Biological Sciences Start-up Funds.

Age and sex have significant impact on microglia morphology: modulation by acute LPS challenge

Jenna Wilson
University of Georgia

Microglia are the resident innate immune cell of the central nervous system and exhibit not only functional, but also morphological changes that are influenced by various factors such as age, sex, and inflammatory stimuli. Functionally, microglia were characterized into three separate states, one unreactive (M0) and two reactive: a pro-inflammatory M1, and an anti-inflammatory M2 state. However, recently, the M1:M2 activated states paradigm has been suggested to be an oversimplification; *in vivo* work has shown that microglia often undergo transition states. The role that age and sex play in microglia function has been investigated to some extent, but associated morphological changes have either been evaluated within males (effect of age), or in adults (effect of sex); detailed, side-by-side comparisons between males and females at different ages are yet to be done. Additionally, effects of chronic inflammation subsequent to an inflammatory challenge or an infection on microglia morphology has been studied but effects of acute challenges have not. Adult (4-5 months old), middle-aged (14-15 months old), and aged (20-21 months old), C57BL/6J male and mice with GFP-tagged microglia (on the CX3CR1 locus) were challenged with LPS (*Escherichia coli* 0111:B4, 0.3 mg/kg, i.p.) or saline vehicle. Four h post, mice underwent open-field behavioral testing; 6 h post, brains and plasma were harvested. Brains were fixed, sectioned, and processed for image analyses of hippocampal GFP+ microglia morphology by detailed Sholl and fractal analyses and appropriate statistics. Selected plasma cytokines were analyzed by a multiplex assay. Overall, age exerted strong influence on microglia morphology, with measured reductions in branch complexity and length, soma circularity, and the density of the cell, accompanied by increases to soma size and cellular elongation. Adult female microglia had more branches, intersections, and branch length than adult male microglia; they were also more responsive to LPS, which decreased these parameters only in the adult females. Total branch length in the middle-aged females was greater than in males and their microglia were more ramified; LPS decreased soma circularity in both sexes during middle age; beginning at middle age, microglia of mice from both sexes exhibited age-dependent decreases of intersections, soma circularity, fractal dimension and branch length; soma area increased only in the aged mice and cell density was the lowest in middle-aged mice. Behaviorally, LPS elicited sickness behavior (decreased horizontal and, especially, vertical activity) at all ages; the effect was progressively stronger with age and, females, adult females in particular, were affected more than their male counterparts. In the plasma, LPS increased all measured cytokines in both sexes and at all ages. Notably, the increases were age-dependent and the highest levels were observed in the aged mice. Additionally, with the exception of IL-6 (middle-aged and aged mice) and CXCL-1 (aged mice) post-LPS levels, all other cytokines increased significantly more in the female mice. In the absence of LPS challenge, cytokine levels were

markedly lower, though still present, with analysis is still ongoing. Nonetheless, some anti-inflammatory cytokines, such as IL-5, IL-4, and IL-10, trended higher in females across ages. Collectively, these findings demonstrate that microglia morphology is affected by not only age, but by sex as well, with the middle-age representing a critical transitional stage. The morphological differences found herein suggest that microglia contribution to brain health and pathology is skewed towards pathology by aging beginning at middle age, with more amoeboid microglia than in earlier stages of life. This shift to more amoeboid morphology is also accompanied by a shift to more rod-shaped morphology, highlighted by increased elongation and decreased primary branches and interesections, which further indicates pathology. Additionally, acute inflammatory stimuli might be more consequential in females, at least earlier in life, both behaviorally, and morphologically. Furthermore, the female-biased peripheral cytokine increase suggest that females are more responsive to acute inflammatory challenge systemically. However, along with age-dependent microglia changes, concomitant increases of anti-inflammatory cytokines, such as IL-10, especially later in life, precludes greater LPS effects in females compared to males on microglia morphology in older mice. This research was made possible by in part by NIH/NIEHS under project number R21ES026383 as well as funding from the Lalita and Raghubir Sharma Distinguished Professorship in Toxicology (NMF) fund.

Sponsors:

UL Research Institutes | Chemical Insights

Department of BIOLOGICAL SCIENCES Clemson University

College of SCIENCE

PhD Poster Abstracts

Exploratory Assessment of Preconception Phthalate Exposure on Fertility and Offspring Health in Mice
Maryam Afghah
Clemson University
Infertility affects 10–15% of couples worldwide and is increasingly attributed to environmental exposures, particularly endocrine-disrupting chemicals (EDCs) such as phthalates. Phthalates are a class of EDCs that are well known for their reproductive toxicity and are of particular concern for women's reproductive health due to their prevalence in personal care, beauty, and feminine hygiene products. To date, our mechanistic understanding of reproductive susceptibility to phthalates has primarily focused on exposure during gestation and early postnatal development and little is known about how preconception exposures influence fertility and offspring health. To address this knowledge gap, we sought to characterize the physiological consequences of preconception phthalate mixture exposure on maternal and offspring health outcomes. Thus, we hypothesize that preconception phthalate exposure will disrupt hormone dependent processes including the estrus cycle and implantation, leading to downstream consequences for placental architecture and function and offspring health. Female CD-1 mice were orally exposed to vehicle (corn oil) or an environmentally relevant mixture of phthalates (200 µg/kg BW/day) from postnatal day (PND) 30-60. Twenty-four hours after their final dose they were paired with a male until they presented with a sperm plug, designated embryonic day (E) 0.5. Pregnant females were then split into three cohorts to evaluate impacts on: (1) implantation (E5), (2) fetal and placental development (E14.5), and (3) adult offspring health outcomes (PND 60). Maternal body weight and estrus cycle were tracked throughout the duration of exposure. Implantation sites were counted at E5 using Chicago Blue stain administered via tail vein injection. Litter size was counted, and fetal and placental weights were collected at E14.5 Adult offspring bodyweight and estrus cycle were tracked between PND 30-60 and liver were collected at PND 60 for both sexes. RNA-seq at E14.5 placentas and PND 60 liver of offspring was performed for both sexes. Phthalate exposure altered estrous cyclicity, with dams spending more time in proestrus and less in metestrus but did not significantly impact implantation or litter size. At E14.5, exposed fetuses exhibited increased bodyweights, accompanied by an expansion of the placental junctional zone in males. Altered bodyweight persisted into adulthood, however adulthood offspring displayed a reduction in bodyweight. RNA-sequencing revealed widespread transcriptional reprogramming in female placentas (518 DEGs) affecting immune regulation, steroid metabolism, and extracellular matrix remodeling, while male placentas exhibited only 9 DEGs but showed structural alterations. In offspring livers, transcriptomic shifts were sex- specific: females displayed downregulation of metabolic and immune genes (e.g., *Cyp7a1,Mthfr, H2-DMB1*), while males showed upregulation of hepatic signaling capacity and reduced adaptability to stress (e.g., *Elf4, Adm2, Ly6a*). Collectively, these findings demonstrate that preconception phthalate exposure induces subtle but biologically meaningful maternal endocrine disruption, alters placental structure and function, and reprograms offspring growth and liver transcriptomes in a sex-specific manner. This work identifies the preconception window as a critical period of vulnerability for EDC impacts on reproductive success and intergenerational health.

Acute Exposure to PEGylated Gold Nanoparticles Cause Mitocondrial Dysfunction: The Role of AuNPs' shape
Bruce Andriolo
Auburn University
Gold nanoparticles (AuNPs) with tunable physicochemical properties have emerged as promising candidates for the treatment of chronic diseases, including cancer and neurodegenerative disorders. Despite explored in clinical trials, there is no gold-based nanoplatforms approved. Due to their inorganic nature, the potential toxic effects of AuNPs, which is often related to their properties such as size, surface chemistry and shape, is a concern. As central hubs of cellular physiology, mitochondria play a pivotal role in health and disease. The impact of AuNPs on mitochondrial-related parameters are still understudied. Therefore, this study aims to

assess the mitochondrial impact of AuNPs with different physicochemical properties in HMC3 human microglial cells, a relevant model for investigating brain function and health. Cells were exposed for 24 hours to a low dose of 0.5 nM of four well-characterized AuNP types: citrate-capped nanospheres, PEGylated nanospheres, PEGylated nanorods, and PEGylated mini long nanorods. These surface chemistries were chosen due to their widespread use in nanomedicine and AuNPs present in consumer products. Particles were well- characterized in both water and complete media by UV-Vis spectroscopy, dynamic light scattering, and zeta potential. None of the AuNPs induced cytotoxicity or impaired cell proliferation, as assessed by viability and proliferation assays up to 72 hours. However, flow cytometry measurements showed that PEGylated nanorods significantly increased cellular reactive oxygen species (ROS), a non-significant increase in mitochondrial ROS, and caused a significant reduction in mitochondrial membrane potential, features of mitochondrial dysfunction, in HMC3 cells following acute exposure (24 h). Mitochondrial respiration profiling via the Seahorse XFe96 Analyzer revealed that acute exposure to PEGylated nanorods also reduced basal respiration by approximately 42%, indicating disruption of oxidative phosphorylation and a potential shift in cellular metabolism. These findings suggest that anisotropic PEG-coated nanorods, despite being non-cytotoxic, lead to significant mitochondrial stress. Our findings highlight the need to consider particle shape and surface chemistry in the design of AuNP-based applications. Moreover, mitochondrial impairment in microglial cells have broader implications for neuroinflammation and neurodegeneration, especially under chronic exposure conditions. Given the growing interest in employing AuNPs to treat diseases, including mitochondrial dysfunction related-diseases, our findings underscore the critical need for detailed mechanistic studies evaluating mitochondrial effects in brain-relevant models.

Investigation of adverse effects of long-term exposure to e-cigarette compounds in human cardiomyocytes

Cameron Brown
Clemson University

Electronic cigarettes (e-cigarettes) have garnered popularity as a “healthy” alternative to traditional cigarette smoking, though evidence suggests that e-cigarettes pose their own unique risks to the cardiovascular system. As one of the major compounds in e-cigarettes, nicotine has been shown to induce oxidative stress, impair mitophagy, and promote apoptosis, all of which contribute to the pathology of cardiovascular diseases. However, there remains a knowledge gap in the understanding of e-cigarette toxicity in cardiomyocytes (CMs) due to methodological shortcomings in the existing literature that do not reflect real-world e-cigarette use. Notable deficiencies include the use of supraphysiological chemical concentrations, unrealistic and unrepresentative chemical compositions, short-term exposure regimes, and non-human models. This study aimed to address these shortcomings by investigating the individual and synergistic cardiotoxic effects of mainstream e-cigarette chemicals on hiPSC-derived CMs under clinically relevant exposure conditions. After 2 weeks of exposure to physiologically relevant combinations and concentrations of freebase nicotine (L-nicotine), salt nicotine (nicotine benzoate), and propylene glycol (PG), we evaluated mitochondrial and cardiac functions and performed transcriptomic analyses of the treated CMs. We found that the nicotine-derivatives or PG alone did not induce obvious adverse effects; while when CMs were exposed to nicotine and PG in combination, they exhibited dysfunction. We also found that salt nicotine was more cardiotoxic than freebase nicotine, and the mixture of nicotine salt and PG induced the greatest dysfunction of all treatment groups. Overall, we concluded that modern-era, pod-based e-cigarettes formulated with nicotine salts induce greater cellular dysfunction in CMs than tank-based electronic smoking devices with freebase nicotine.

Genomic Characterization of Human in Vitro Derived Spermatids

Arina Chernikova
University of Georgia

In vitro spermatogenesis (IVS) aims to replicate sperm development in culture but faces major challenges such as recreating a testis-like microenvironment, maintaining the viability and maturation of every germ-line and somatic cell type involved, and driving the process to completion so that fully functional sperm are produced.

Two persistent hurdles have limited human in vitro spermatogenesis: 1) confirming that laboratory-derived spermatid-like cells can fertilize oocytes and give rise to healthy progeny, and 2) demonstrating that meiosis/meiotic crossing-over in culture recapitulates processes observed in vivo. Our lab has recently demonstrated, using non-human primate pluripotent stem cells, that functional spermatids can be generated in vitro that can fertilize non-human primate oocytes and produce healthy embryos, although healthy progeny have not yet been produced. While generating healthy progeny is underway, we have begun assessing the second hurdle listed above by performing genome-scale characterizations of human spermatids produced in a novel in vitro stepwise co-culture in vitro spermatogenesis system that more closely mimics the testicular microenvironment. While our new in vitro culture system shows increased expression of key meiotic genes/proteins and simulates stages of meiosis I, definitive proof of crossing-over has not been achieved. Here, in vitro-derived spermatids with a 1C DNA content were isolated by FACS, subjected to whole-genome amplification, and sequenced with single-molecule PacBio HiFi reads. In parallel, the parental, diploid H14 (WA14) line was sequenced, with a de novo MaSuRCA assembly now serving as a reference for ploidy validation and crossover mapping in haploid spermatid-like cells. By aligning haploid HiFi reads to the parental assembly, we now have evidence of potential crossover events in addition to further confirming haploidy. Establishing an in vitro spermatogenesis model that undergoes authentic in vivo-like recombination will not only clear a path toward regenerative treatments for male-factor infertility, but will also provide a platform for fertility preservation, drug discoveries and toxicological testing.

PFOS perturbs skeletal muscle and liver mitochondrial pathways and lipid and glucose metabolism in vitro: skeletal muscle is more sensitive to PFOS than liver.

Jazmine Eccles-Miller
Clemson University

Background and purpose: Obesity and non-alcoholic fatty liver diseases (NAFLD) are endemic in the United States and many other countries. PFOS is a forever chemical and endocrine disruptor associated with NAFLD and obesity. However, few studies have investigated the effects of PFOS on skeletal muscle, a healthy bodies largest metabolic organ. Skeletal muscle presents a target for PFOS-induced mitochondrial toxicity due to its high mitochondrial content and ability to use multiple energy sources. Mitochondria are considered a likely target for PFOS toxicity and muscle wasting was reported in mice from our laboratory and others. Therefore, we aimed to evaluate and compare the responses of skeletal muscle and liver to PFOS exposure in vitro. **Methods:** C2C12 skeletal myoblasts and HepG2 hepatocarcinoma cells were exposed to PFOS of varying concentrations ranging from 0 to 6 micromolar, followed by assays to evaluate mitochondrial function, fatty acid and glucose metabolism, gene expression, triglyceride accumulation, and oxidative phosphorylation (OXPHOS) complex protein expression. **Results:** PFOS decreased several parameters of mitochondrial respiration, including basal respiration, in C2C12 cells; these parameters were unchanged in HepG2 cells. Spare respiratory capacity was slightly increased in both cell types. PFOS reduced fatty acid metabolism in C2C12 cells but did not alter fatty acid metabolism in HepG2 cells. PFOS increased several measures of glucose metabolism in C2C12 cells; HepG2 cells showed no change in glucose metabolism, rather they showed an increase in non-glycolytic acidification. PFOS decreased triglyceride accumulation in C2C12 cells but increased accumulation in HepG2 cells. RNAseq was performed on C2C12 cells because of the significant metabolic changes observed following PFOS exposure. A significant number of differentially expressed genes (DEG) were identified, and GO term and KEGG pathway analysis showed an increase in expression of genes related to metabolism, including fatty acid and carbon metabolism. RNAseq also showed increased expression of genes related to the AMPK pathway, a pathway largely responsible for regulating catabolism. Downregulated terms included those related to skeletal muscle contraction and cytoskeleton, as well as branch-chain amino acid metabolism. qPCR was performed for HepG2 cells. PFOS did alter expression of several genes in HepG2 cells, including SREBP1c, FASN, and SCD1, and these changes were weak compared to DEG seen in C2C12 RNAseq analysis. Western blots to identify potential changes in OXPHOS complex protein expression showed a significant decrease in complex I protein expression in both C2C12 and HepG2 cells. **Conclusion:** C2C12 cells, an in vitro model for skeletal muscle, are more sensitive to PFOS treatment than HepG2 cells, an in vitro model for the liver. Mitochondrial dysfunction

Sponsors:

and changes in substrate metabolism were observed in C2C12 cells, but these same changes were not observed in HepG2 cells. This suggests the mechanism of toxicity of PFOS varies significantly between these organs, and skeletal muscle is important in understanding the whole-body metabolic dysfunction associated with PFOS exposure. Further investigation should be performed to elucidate a mechanism underlying these changes in skeletal muscle, with particular interest on the AMPK pathway, to understand its contribution to metabolic diseases associated with PFOS exposure.

Sexually Dimorphic Xenobiotic Transport in Human Placental Barrier Modeled by Primary Cytotrophoblast Culture

Ansley Elkins
Clemson University

Nine out of ten pregnant women in the United States have reported taking at least one pharmaceutical drug during their pregnancy. The placenta serves as a biological and chemical barrier that separates maternal and fetal blood supply. While most drugs can cross the placenta barrier via passive diffusion, the placenta also expresses a variety of drug transporters that play a crucial role in fetal drug exposure. Previous research has shown that fetal sex dictates both placental and fetal exposure to xenobiotics. However, the effect fetal sex has on ATB-binding cassette (ABC) efflux transporters and solute carrier (SLC) transporters within the human placenta remains unknown. We hypothesize that sex differences in teratogenicity of xenobiotics are, in part, dictated by sex specific expression and/or activity of these transporters within the placenta. Through our lab's partnership with Prisma Health Greenville Memorial Hospital, we have collected biopsies from human placenta samples that were delivered via cesarean section. Primary cytotrophoblast cells were isolated from these tissues using enzymatic digestion followed by immunomagnetic separation. Quantitative real-time PCR (qRT-PCR) was used to analyze the expression of fifteen major drug transporters. Additionally, eFLUXX assays were preformed to investigate the functional activity of three major transporters (Mrp, Mdr1, and BCRP). Although we have not yet observed a significant difference in transporter activity between male and female placenta samples, we are still in the process of collecting and analyzing samples. Collectively, this work will advance the field's knowledge about biological factors that may contribute to differences in male and female vulnerability to xenobiotics *in-utero*.

Assessing the effects of *p,p'*-DDE, PCB153, BDE47, and PFOS mixtures on adipocytic differentiation of 3T3-L1 cells

Melanie Garcia
Clemson University

Background/Purpose: Obesogens are chemicals that cause weight gain. p,p'-DDE, PCB153, BDE47, and PFOS are known obesogens that have been shown *in vitro* to increase lipid accumulation when exposed individually. We are exposed to these chemicals through the usage of household and personal care products, improper disposal of hazardous waste, and industrial spills. However, we are rarely exposed to just one chemical at a time, so it is imperative to be able to examine real world mixtures. In this study, we used chemical concentration data from maternal serum collected during the first trimester from mothers enrolled in the Environmental Influences on Child Health Outcomes-Fetal Growth Study (n = 813). **Methods:** A self-organizing map (SOM) was applied to prenatal serum concentrations from the ECHO cohort to create five chemical mixtures, or profiles. The profile mixtures consist of four known obesogenic chemicals (p,p'-DDE, PCB153, BDE47, and PFOS) at their real-world serum concentrations (1x Concentration). Preadipocyte 3T3-L1 cells were exposed to the five profiles at 1X, 50X, and 500X concentrations continuously over a 14-day differentiation period into adipocytes. On day 14, cells were assessed for lipid accumulation, adipogenic transcript levels (*Pparγ*, *Lpl*, *Fabp4*, *Cpt1*, and *Fsp27)*, and protein levels of Ampk and Lpl. Protein levels of nuclear Pparγ were assessed at day 7. **Results:** The results indicate that a mixture dominated by high BDE47 levels (Profile 3) behaved differently at 1X, 50X, and 500X concentrations than the 500X concentration of BDE47. BDE47 alone increased expression of *Fsp27*, *Fabp4*, and *Cpt1* by 2.6, 4.5, and 3.5-fold respectively while the Profile 3 mixture inhibited expression of these three genes. Proteins levels of Lpl were significantly decreased in both Profile 3 and BDE47 at 500X, but there were no significant differences in Ampk or Pparγ. Additionally, there were no changes in lipid

accumulation. In contrast, mixtures dominated by either *p,p'*-DDE or PFOS (Profiles 1 and 4) behaved similarly to their dominant chemicals for both mRNA and protein expression levels of Lpl. There were no changes in protein levels of Ampk, but there was an increase in Pparγ in 500X PFOS by 1.8-fold. Lipid accumulation levels were elevated in Profile 1 at the 50X and 500X, p,p'-DDE at 500X, and the 1X concentration of Profile 4 by 1.3-, 1.4-, 1.4-, and 1.3-fold respectively. **Conclusions:** The lipid accumulation, qPCR data, and protein data indicate that the Profile 1 mixture at the 500X concentration and p,p'-DDE at 500X behave similarly. In contrast, Profile 3 exhibits differential effects of mixture profiles on adiposity with mixtures containing relatively high concentrations of BDE47 having antagonistic effects. Such findings illustrate the importance of identifying and investigating toxic effects of real-world mixture exposures.

Low dose exposure to Dihydroxyacetone (DHA) changes to cardiac metabolism and induces DNA damage

Hailey Levi
University of Alabama at Birmingham

Background and Purpose: Electronic cigarettes (e-cigarettes) have become increasingly popular in the last decade and evolved with various devices and e-liquid components. E-liquids are heated to create the aerosol the user inhales, and dihydroxyacetone (DHA) is produced by the oxidation of glycerol in the e-liquids. DHA is also an active ingredient in sunless tanning products. While DHA is considered safe for external exposures, the inhalation exposure risk from vaping and spray tanning has raised concerns about internal exposures to DHA. DHA exposure levels vary between e-cigarette devices with micromolar to low millimolar doses potentially inhaled. Once inhaled and absorbed by cells, DHA is incorporated into several metabolic pathways through its conversion to dihydroxyacetone phosphate (DHAP). Given this metabolic incorporation, DHA exposure effects to highly energetic tissues like the heart are needed. Methods: We exposed human cardiomyocytes (AC16) to multiple doses of 0.2mM DHA over 2, 4, and 8 weeks, then analyzed DNA lesion content and changes in DNA repair proteins. We also examined mitochondrial and metabolic changes utilizing immunoblotting, qPCR, and fluorescent microscopy. In parallel, we sub-acutely exposed A/J mice to 5 µg of DHA by nose-only inhalation daily for 14 days. Echocardiograms were used to assess cardiac function at the end of the exposure period. Using cardiac tissues from these mice and their saline exposed controls, we examined changes in mitochondria number and content, using TEM to look at structure and counts, and qPCR for mitochondrial dynamics and mitochondrial DNA copy number. We also examined collagen using Masson trichrome staining within the cardiac tissues and changes in pro-inflammatory markers and metabolites in plasma and bronchoalveolar lavage fluid (BALF). Results: In AC16 cells, we found an increase in mitochondrial copy number after 2 weeks of exposure to 0.2 mM DHA. At 4 weeks of exposure, we see a decrease in mitochondrial copy number, which then increase again at 8 weeks compared to time-matched control cells. We also see changes in mitochondrial protein measurement changes over these same time period, suggesting duration of DHA exposure induces adaptive changes within the mitochondria. Additionally, we found that there is an increase in oxygen consumption, increased levels of mitochondrial proteins and mitochondria number in exposed cells after two weeks. However, we see these trends changing over the exposure period, with a sudden decrease at 4 weeks but a return of 8 weeks. We also observed an increase in oxidative and alkylation DNA lesions over the exposure periods with levels of DNA damage changing over time. Interestingly, there is a shift in the DNA lesion profile across 4 and 8 weeks of DHA exposure with altered levels of DNA crosslink-type lesions and uracil content. In the mice, we saw a significant increase in mitochondria DNA copy number and mitochondria number in male and female mice 2 weeks after daily exposure to 5 µg DHA. Additionally, we saw an increase in pro-inflammatory markers, most notably IL-6, in the female mice. However, when we looked at collagen levels, we saw an increase in collagen in the males only, with no change in the females. Echocardiograms revealed an increase in ejection fraction and fractional shortening in the males, but a decrease in the females. There was also an overall increase in global stain, suggesting that the males are undergoing cardiac hypertrophy and the females are undergoing cardiotoxicity. Conclusion: This work is the first to examine genotoxicity of DHA in cardiomyocytes and characterize physiologically relevant exposures in animals to understand potential long-term effects on cardiovascular health. Additionally, this is the first time sex specific responses to DHA exposure were observed.

Sponsors:

Using human-induced pluripotent stem cell derived motor neurons to assess a critical period of susceptibility to sodium arsenite during development

Erin Levon
Clemson University

Background/purpose: Arsenic is a toxic metalloid that enters groundwater through erosion. It is known that arsenic levels can exceed the 10 ppb limit established for drinking water in the United States, and chronic arsenic exposure affects as many as 150 million people worldwide. Arsenic has been shown to impair neuronal and skeletal muscle development, so it is important to understand how chronic arsenic exposure may affect motor neuron development. **Methods:** Human-induced pluripotent stem cells (iPSCs) were differentiated over 28 days to mature motor neurons. During differentiation, iPSCs were exposed to 37.5 ppb (0.5 µM) of arsenic at different developmental time points: days 0-6, days 0-12, days 0-18, days 0-28, days 6-28, days 12-28, and days 18-28, to assess a critical period of susceptibility. Exposure times were based on important periods of development during a previously established differentiation protocol, where iPSCs are differentiated to neural epithelial progenitor cells at day 6, motor neuron progenitor cells at day 12, early motor neurons at day 18, and mature motor neurons at day 28. On day 28, RNA was extracted to assess mRNA transcript levels for markers of motor neurons at very early stages of development (*SOX1, OLIG2, NES),* markers of mature cholinergic motor neurons (*CHAT, CHT, VACHT, ACHE, CACNA1A)*, a marker of dopaminergic neurons (*TH),* a marker of glial cells (*GFAP),* and a marker of mature glutaminergic motor neurons (*VGLUT1).* **Results:** Cells that were exposed to arsenic between days 0-12 of motor neuron differentiation showed significant upregulation of mRNA transcripts for acetylcholinesterase (*ACHE*), choline acetyltransferase (*CHAT*), choline transporter (*CHT*), vesicular acetylcholine transporter (*VACHT*), and calcium voltage-gated channel subunit alpha 1A (*CACNA1A*) compared to groups exposed to arsenic later in differentiation. *NES* and *OLIG2,* early markers of differentiation, were significantly reduced in almost all motor neuron groups exposed to arsenic between days 0 and 6, indicating that early differentiation is the stage most impacted by arsenic. As expected, both *TH* and *GFAP* were not present in the samples, but there were significant increases in expression of *GLS1* and *vGLUT1* in 28 day motor neurons exposed to arsenic. **Conclusions:** Overall, these results indicate that the critical period of arsenic toxicity is between days 0 and 12 of motor neuron differentiation. Further, most of the genes in the acetylcholine pathway transcripts were affected similarly, and genes for glutamatergic neurons were increased, indicating that arsenic exposure affects the overall ability of the motor neurons to differentiate appropriately as opposed to targeting a specific portion of the acetylcholine cycle.

Polyvinyl chloride nanoplastic induces mitochondrial damage in human cardiomyocytes

Xiao Li
Clemson University

Background: In recent decades, plastic has become one of the indispensable materials in human life.[1] Its advantages of light weight, low cost, and bio-inertness have led to its widespread use in food packaging, cosmetics, and industrial products.[2] The main plastic materials present in the environment include polystyrene (PS), polyvinyl chloride (PVC), polyethylene (PE), and polypropylene (PP).[3] Numerous studies have indicated that plastics experience ageing under natural conditions, leading to an enhancement of their toxicity.[4] Plastics can be absorbed by humans via ingestion, inhalation, or dermal contact, potentially causing a variety of adverse health effects.[5] PVC is among the most biologically toxic substances on earth, releasing harmful chemicals throughout its lifecycle. These toxins can bioaccumulate in the food chain, eventually posing risks to human health.[6] A study of 304 patients with cardiovascular disease reported that PE was present in the carotid plaques of 58.4% of participants, and measurable PVC was detected in 12.1% of them.[7] Microplastics(MPs) are generally defined as particles with a diameter smaller than 5 mm, while nanoplastics(NPs) are those with a diameter smaller than 1 µm.[8] NPs present in aquatic environments tend to bioaccumulate in aquatic organisms, resulting in toxic effects such as growth and developmental inhibition, oxidative stress, and dysregulation of the immune system.[9] NPs are capable of crossing barriers like the intestinal epithelium and the blood-brain barrier, posing potential risks to human health.[10] Particles with sizes below 400 nm have the potential to traverse biological barriers, including the human term placenta, and be systemically absorbed.[11] Studies indicate that MPs tend to

accumulate in multiple human organs, particularly the lungs, liver, and heart.[8,12] Cardiovascular disease (CVD) represents a significant global health issue, and studies have noted that the presence of MPs in patients with carotid artery disease correlates with a higher likelihood of death.[13] Nevertheless, studies investigating the impact of MPs on cardiac health and their related risks are still limited.[14] In rat studies, MPs have been found to harm cardiac mitochondrial structure and function, leading to a loss of mitochondrial integrity.[15,16] One embryonic study in zebrafish has shown a significant downregulation in the expression of genes associated with cardiac development.[17] Another study in mouse cardiomyocytes indicates that MPs can promote oxidative stress, which in turn leads to apoptosis.[18] Research indicates that microplastics and nanoplastics (MNPs) may induce cardiotoxicity through mitochondrial dysfunction, manifested as reduced mitochondrial membrane potential, increased mitochondrial reactive oxygen species (ROS), and elevated intracellular ROS levels.[19] **Purpose:** To date, most studies on NPs have concentrated on PS, with research on PVC being extremely limited. A study in mouse cardiomyocytes indicated that PVC NPs can enter cardiomyocytes and causing mitochondrial dysfunction.[20] The present study aims to investigate the functional and mechanistic impacts of PVC NPs on human-induced cardiomyocytes, with a specific focus on elucidating the mechanisms underlying mitochondrial dysfunction. **Methods:** Human embryonic stem cells were differentiated into cardiomyocytes using a small-molecule protocol, with spontaneous beating typically observed by day 7. Cardiomyocytes were then exposed to polyvinyl chloride (PVC) nanoparticles of varying sizes and concentrations to assess cellular responses. Cell viability, contractile function (live-cell video recording), calcium transients (Fluo-4 imaging), and apoptosis were evaluated. Mitochondrial function and morphology were further examined using Seahorse XF mitochondrial stress testing, MitoTracker staining, and transmission electron microscopy. At the molecular level, Western blotting was performed to analyze autophagy-related proteins (LC3-I/II), with GAPDH as the loading control. Data from imaging, flow cytometry, and functional assays were quantified using ImageJ, MATLAB, FlowJo, and Seahorse Wave software. Together, these approaches systematically characterized the effects of PVC nanoparticles on cardiomyocyte viability, contractility, calcium handling, mitochondrial function, and autophagy. **Results:** H1 human embryonic stem cells were efficiently differentiated into cardiomyocytes, which displayed spontaneous beating by day 7. Upon exposure to PVC nanoparticles, cardiomyocytes exhibited size- and concentration-dependent cytotoxicity, with smaller particles showing stronger inhibitory effects. Functional assays demonstrated that PVC treatment led to irregular and weakened calcium transients, reduced contraction amplitude, and disordered beat frequency, indicating impaired calcium handling and contractile dysfunction. Seahorse analysis further revealed decreased oxygen consumption and impaired oxidative phosphorylation, while MitoTracker staining showed increased mitochondrial fragmentation. Western blotting confirmed an elevated LC3-II/LC3-I ratio, suggesting that PVC exposure promotes mitochondrial damage and activates autophagic processes. **Conclusion:** Our study demonstrates that PVC nanoparticles exert size-dependent cytotoxic effects on human-induced cardiomyocytes, with smaller particles exhibiting higher toxicity. PVC exposure disrupts calcium homeostasis and contractile function, as evidenced by irregular calcium transients and reduced contraction amplitude, indicating impaired excitation-contraction coupling. Additionally, PVC treatment compromises mitochondrial function, leading to decreased oxygen consumption, enhanced mitochondrial fragmentation, and disturbed mitochondrial dynamics. Importantly, PVC exposure also elevates the LC3-II/LC3-I ratio, suggesting activation of autophagy in response to cellular stress. Together, these findings provide mechanistic insight into PVC nanoparticle–induced cardiotoxicity, highlighting the potential risks of environmental PVC exposure to human cardiac health.

Metabolomic shifts in beef steers rotationally grazing toxic endophyte-infected tall fescue under fall conditions

Ignacio Llada
University of Georgia

Research background and purpose: Fescue toxicosis (FT) is a worldwide mycotoxicosis caused by ingestion of tall fescue infected with the ergot alkaloid (EA)-producing endophyte *Epichloë coenophiala.* The EAs, such as ergovaline, produced by this endophyte, are affecting animal health by mimicking the action of biogenic amines. While the vascular system is a major target, the broad receptor distribution for these amines suggests wider

physiological effects. This study aimed to holistically characterize EA-induced metabolic disruption in steers under fall rotational grazing conditions. Our objectives were to identify a) altered metabolic pathways, b) metabolic features with exposure/effect biomarker potential, c) prevalent EA across matrices, and d) characterize the dynamics of volatile fatty acids (VFAs) in the rumen fluid of steers grazing toxic pasture. **Materials and methods**: Eighteen steers grazed nontoxic, toxic (E+), or endophyte-free fescue pastures. After 14 days, groups switched diets (toxic to nontoxic and vice versa). Urine, saliva, plasma, and rumen fluid (RF) were collected before (pre), 2, 7, 14, 21 and 28 days after pasture allocation. Untargeted, high-resolution metabolomics (HRM) analysis was performed on all matrices and processed using MetaboAnalyst 6.0. VFAs concentrations in RF were quantified via gas chromatography–mass spectrometry (GC-MS). **Results**: Total and individual VFA concentrations (acetate, propionate, butyrate, valerate) increased in RF during E+ exposure ($P \leq 0.05$) and returned to baseline after removal. sPLS-DA analysis of both 14-day periods showed a clear groups separation based on metabolic features detected using HILIC and C-18 columns. Discriminatory E+ features followed a distinct pattern: pre-pasture placement showed no differences ($P > 0.05$), but intensity increased, becoming significant ($P \leq 0.001$) on days 2, 7, and 14. A switch to non-toxic pastures led to return to baseline levels within two days. Key affected metabolites included tyramine, methyltyramine, methoxytyramine, dopamine, indoleacetic acid, among others. Pathway analysis indicated downregulation of beta-oxidation, fatty acid, and arachidonic acid metabolism in E+ steers, while aromatic amino acids (e.g., tyrosine, tryptophan), non-aromatic amino acid (e.g., lysine, branched-chain amino acids), vitamin B6, and carbohydrate metabolism (e.g., glycolysis, gluconeogenesis) were upregulated. Upregulated pathways were mostly amino acids (45%), while downregulated were mainly lipids (60%). Clavine alkaloids, and lysergic acid derivatives (e.g., ergine, lysergol) were the primary EAs detected in the urine, saliva, and RF, but not in the plasma of E+ steers, rising sharply within two days of exposure, remaining elevated, and returning to control levels within two days after removal from E+ pastures. **Conclusions:** Increased VFAs concentrations in RF suggest impaired absorption, likely from reduced ruminal motility and/or EA-induced vasoconstriction on ruminal vessels. This would limit the absorption of gluconeogenic and energy substrates, possibly driving E+ steers towards alternative energy sources to meet demands, e.g., a shift towards greater dependence on amino acids. The observed downregulation of lipids and upregulation of amino acid and carbohydrate pathways (e.g., gluconeogenesis) indicate that E+ grazing disrupts energy metabolism, shifting utilization from lipids toward amino acids. Simple ergoline alkaloids were the main circulating EAs, suggesting ruminal ergopeptines biotransformation. Upregulation of the vitamin B6 pathway, together with increased biogenic and trace amines in RF of E+ steers, implies that EAs ingestion may selectively enrich ruminal microbes capable of their biotransformation, which also express pyridoxal phosphate (vitamin B6)-dependent aromatic amino acid decarboxylases that convert aromatic amino acids into these bioactive compounds. These molecules, alone or combined, may contribute to FT pathogenesis, highlighting the need for further research into their biological effects. **Financial Support:** U.S. Department of Agriculture. Grant Number 67015-31301.

Behavioral effects of polystyrene microplastic exposure in zebrafish (Danio rerio) larvae

Carlos Lopes
Auburn University

Microplastics (MPs) are microscopic plastic particles that commonly originate from the breakdown of plastics. Their ability to cross biological barriers, bioaccumulate, and transport harmful agents poses a risk to exposed organisms. However, effects of MPs during developmental stages remain poorly understood. Thus, we aim to describe the effects of two different MPs on zebrafish larval behavior. At twenty-four hours post fertilization (hpf), embryos were mechanically dechorionated, and exposed to 0, 0.1, 1, or 10 µg/ml of MP solutions derived from disposable red plastic drinking cups (solo cups) or plastic forks. Larval behavior was monitored in response to light and tapping stimuli at 120 hpf. For the visual motor response (VMR) test, larvae were exposed to a series of 10-minute periods that alternate between dark and light for a total of 50 min. Data for movement endpoints such as distance moved, velocity, time spent moving, turn-angle, angular velocity, mean meander, and turning direction were collected. For the tapping response test, a solenoid inserted at the bottom of the base of the behavior chamber was used for mechanical stimulation. Each trial consisted of 10 min of acclimation, followed

by a single tap (level 8 [most intense]), to elicit startle responses in darkness. For startle responses, the same movement endpoints were analyzed over a period of 3 s after the tap. We found no statistically significant differences in behavior after the tapping stimulus for both MP solutions. In the VMR assays, MP exposure induced source- and concentration-dependent behavioral effects in zebrafish larvae. Fork MPs promoted hyperactivity at low concentration (1 µg/ml) but reduced locomotion and angular activity at higher concentration (10 µg/ml), whereas cup MPs predominantly impaired locomotion and turning behaviors across concentrations. These findings indicate that MP origin influences toxicity profiles, with distinct behavioral phenotypes emerging from different particle sources.

Novel Function of Emergency Contraceptives in Disrupting Uterine Fluid Dynamics

Taylor Martin
University of Georgia

The signaling of ovarian hormones estrogen (E2) and progesterone (P4) is essential for early pregnancy events. E2 and P4 act primarily through their respective receptors, estrogen receptor alpha (ERα) and progesterone receptor (PR). One of their major functions is regulating the dynamic uterine fluid volume during early pregnancy. Preovulatory E2 signaling stimulates uterine fluid accumulation to facilitate post-coital sperm transport to the oviduct/Fallopian tube for fertilization. Postovulatory P4 signaling promotes uterine fluid reduction for uterine lumen closure, which enables intimate contact between an implanting embryo and maternal uterine luminal epithelium (LE) to initiate embryo implantation. Antagonizing PR to disrupt P4 signaling is a main strategy for hormonal contraceptives, like mifepristone (RU486). RU486 is the most common emergency contraceptive prescribed annually to millions of women worldwide. One RU486 pill commonly contains 200 mg (equivalent to 2~4 mg/kg for a woman in a body weight range of 50~100 kg); up to 800 mg RU486 was used in clinical studies, and up to 1800 mg RU486 was used in a tolerance test. Our dose-response and time-course studies in mice, which have embryo attachment ~day 4.0 post-coitum (D4.0), reveal inhibition of embryo implantation by a single dose of RU486 (2-8 mg/kg) given between D2 @ 9 h and D3 @ 18 h. Additionally, the inhibitive effect of embryo implantation was correlated with excessive uterine fluid retention, prominently in the 4-8 mg/kg RU486 groups. In women undergoing *in vitro* fertilization-embryo transfer (IVF-ET), delayed uterine fluid absorption or uterine fluid retention were correlated with impaired or failed embryo implantation, respectively. We propose uterine fluid retention as a mechanism for RU486 as a contraceptive. Since the uterine epithelium is the gate for uterine fluid movement, and RU486 targets PR for contraception, a uterine epithelial PR knockout mouse model *epiPR*$^{-/-}$ (*Pgr*$^{f/-}$ *Wnt7a*$^{Cre/+}$) is a suitable *in vivo* model for our study. The *epiPR*$^{-/-}$ mice are infertile, with abnormal uterine fluid retention and failed embryo implantation. Intrauterine injection of fluorescent tracer Alexa Hydrazide (AH) reveals reduction of bulk uterine fluid absorption into *epiPR*$^{-/-}$ LE cells on D3.5 @ 17 h compared to that in the *Pgr*$^{f/-}$ control mice, and this reduction of bulk uterine fluid absorption is correlated with fluid retention in *epiPR*$^{-/-}$ uterus. Analysis of publicly available ChIP-seq data reveals binding sites of PR near promoter regions of genes with known functions in fluid movement, such as calcium-activated chloride channel regulator 1 (*Clca1*, for regulating Cl^- absorption), Na^+/K^+ ATPase subunits (*Atp1a1, Atp1b1, Atp1b3,* for Na^+ export through basolateral epithelial membrane), and aquaporin 1 (*Aqp1*, channel for water movement), etc. Na^+ and Cl^- are dominant ions in the uterine fluid. Preliminary immunofluorescence data shows upregulation of CLCA1 but downregulation of AQP4 and ATP1A1 in *epiPR*$^{-/-}$ LE on D3.5 @ 17 h compared to that in control mice. Control mice treated with 200µg of RU486 on D3.5 @ 9 h had reduced bulk uterine fluid absorption and increased CLCA1 expression on D3.5 @ 17 h. These preliminary data implicate P4-PR signaling in uterine fluid movement. We will determine the molecular targets of RU486 in the uterine epithelium for regulating uterine fluid movement.

Altered ovarian steroidogenesis as a mechanism for the effects of endocrine disrupting compounds on the uterus

Kristofer Meier
University of Georgia

The uterus is essential for supporting mammalian pregnancy. Uterine functions are under the master control of ovarian hormones estrogen and progesterone, which act through estrogen receptors (ER) and progesterone

receptors (PR), respectively. Endocrine-disrupting chemicals (EDCs) such as mold-derived mycoestrogens, pesticides, and industrial byproducts can enter the body and disrupt endogenous hormone signaling. We previously demonstrated that exposure to environmental EDCs (e.g., mycoestrogen zearalenone) in mice could disrupt uterine functions in supporting early pregnancy. Despite the essential roles of ovarian hormones in maintaining the uterine environment and known effects of EDCs in disrupting uterine and ovarian function, there is a significant knowledge gap in connecting the uterine phenotype to ovarian effects. We hypothesize that EDCs may dysregulate ovarian steroidogenesis leading to uterine dysfunction. In this study, we treated young adult cycling mice (N=4/group) with RU486 (PR antagonist, 200µg/day), ICI-164384 (ICI, ER antagonist, 20µg/day), and diethylstilbestrol (DES, ER agonist, 0.5µg/day) as model EDCs, and oil as vehicle control. Mice were treated for 4 days and vaginal cytology was surveyed daily to observe estrous stages. RU486- and DES-treated mice experienced an extended estrus while ICI-treated mice had a lengthened diestrus. Mice were dissected 24 h after the 4th treatment. Two sets of ovary and uterine horn were extracted from each mouse; one set was fixed in formalin while the other was flash-frozen. RNA-seq was performed on paired sets of flash-frozen ovary and uterus. Preliminary analysis of ovarian RNA-seq data reveals tissue-specific effects of each treatment on the uterine and ovarian transcriptomes. *Cyp17a1*, which encodes for cytochrome P450 17a1 involving progesterone metabolism, and *Cyp19a1*, which encodes for cytochrome P450 19a1 involving estrogen synthesis, were both differentially expressed across treatment groups in the ovary, while expression is barely detectable in the uterus. One or both genes also show differential expression compared to vehicle-treated groups with similar vaginal cytology/estrous stages, suggesting disrupted steroidogenesis and/or metabolism of ovarian hormones estrogen and progesterone in the ovary upon treatments with model EDCs. Future studies will determine serum estrogen and progesterone levels and employ immunohistochemistry to detect CYP17A1 and CYP19A1 in the ovaries to further validate the RNA-seq data.

Impact of Developmental Exposure to Environmental Levels of PFAS and PFAS Mixtures on Multi-tissue Transcriptomic Profiles in Adult Zebrafish

Alyssa Meyers
University of Florida

Background and Purpose: Concern over the potential effects of per- and polyfluoroalkyl substances (PFAS) commonly present in the environment (including drinking water) have risen since the early 2000s. Although certain PFAS, including perfluorosulfonic acid (PFOS) and perfluorooctanoic acid (PFOA) are no longer used in manufacturing in the United States, they are ubiquitous in the environment due to their strong carbon fluorine bonds rendering them effectively indestructible. PFOA and PFOS have been reported to induce immunotoxicity, endocrine toxicity, and developmental toxicity. Epidemiological studies have associated PFAS with altered immune function, liver disease, lipid metabolism dysregulation, kidney disease, miscarriages, and cancer. **Methods:** In this study, we sought to determine the effect of an environmental level of exposure (70ng/L) of PFOA, PFOS (240 ng/L) , and a mixture (35 ng/L of PFOA + 120 ng/L of PFOS) of each on larval zebrafish from 0-5 days post-fertilization (dpf) that were then raised to adulthood (~18 months. Quant-Seq transcriptomic analyses was then used to analyze extracted RNA from brain, gonad, liver, and kidney tissue of male and female control and exposed fish (n=2- 4/treatment; 4-8/respective control). 3' mRNA-seq libraries were prepared using an Illumina QuantSeq prep kit, sequenced and transcript expression was quantified. Libraries were quantified using a Qubit 2.0 fluorometer and run on an Agilent TapeStation 2200 for quality control. The samples were sequenced on an Illumina HiSeq 2500 and analyzed using a combination of the Lexogen Bluebee Genomics Platform and Lexogen in-house data analysis. Reads were aligned to *D. rerio* (Build GRCz11). Differentially expressed genes (DEGs) were determined via DESeq2 and defined by absolute log2 fold change value $\geq |1|$; $p < 0.05$. DEGs were compared for overlap using UpsetR and were uploaded into Ingenuity Pathway Analysis (IPA). **Results:** Previously, we reported that developmental PFAS exposure altered lipid transcriptomics and light/dark swim distance in larval fish (5 dpf) and impacted fecundity in PFOA-exposed fish raised to adulthood (4-6 months). Although number of DEGs were low in juvenile fish between 1 and 106, adult fish were found to have anywhere from 2-9360 DEGs. IPA analysis of DEGs revealed significant enrichment of a number of disease pathways, including cancer, lipid metabolism disruption, endocrine disruption, organismal survival,

cancer, and reproduction in PFAS exposed fish. More specific outcomes were identified in association with each organincluding motor development and seizure markers in the brain and liver cancer, steatosis and carcinoma in the liver. **Conclusion:** Early life PFAS exposure at environmentally relevant levels has multisystemic effects months after the initial exposure. Ongoing studies are supporting the associated links of PFOA and PFOS in human populations with animal toxicology studies including zebrafish. This research is important to determining the effect of PFAS on public health and the relative safe level of PFAS in drinking water.

Aryl hydrocarbon receptor (AhR2) Signaling Mediates Tetrabromobisphenol A (TBBPA) Toxicity in Zebrafish

Kanchaka Pathirajage
Clemson University

Research Background: Tetrabromobisphenol A (TBBPA) is extensively used in commercial products such as synthetic textiles, plastic paints, and electronic devices to reduce flammability, but can be potentially toxic from indoor exposures. Our prior work using zebrafish as a model shows that 1) at low level exposures, TBBPA induces a myriad of developmental deficits, including increased reactive oxygen species (ROS) as well as disruption of cartilage and blood cell development and - 2) the aryl hydrocarbon receptor signaling is strongly induced in TBBPA treatments. Within this study, we hypothesize that TBBPA-induced developmental toxicity is caused by AHR2 overexpression.**Purpose**:This study aims to leverage zebrafish embryos as a model to study the mechanism of AHR2 signaling on TBBPA induced impacts on cartilage, blood cell production and oxidative stress. **Methods**: At 6 h post fertilization, embryos were exposed to TBBPA (0 or 5 µM), followed by phenotyping, tissue uptake quantification by LC-MS and mRNA seq at 24 hpf. For co-exposure studies, embryos were exposed to 0 or 0.5 µM TBBPA in presence or absence of 1.25 µM GNF- 351- a known AHR inhibitor. Immunohistochemistry for AHR2 (zebrafish functional ortholog of human AHR) and CYP1A proteins as well as CH2DCFDA stain for reactive oxygen species (ROS) were conducted at 24 and 72 hpf. Following this, o-dianisidine assay and Alcian Blue assays were conducted to measure hemoglobin production and cartilage development respectively at 72 or 120 hpf. **Results**: Our LC-MS data showed that tissue uptake at 5 µM is 62 ± 41 ng/g that aligns with environmentally detected levels in serum and cord plasma. mRNA-seq analysis revealed that pathways related to metabolism, stress and lipid transport were disrupted. Specifically, we saw a strong upregulation of AHR2 signaling genes, including *cyp1a* (*log_2 fold change = +6.16*), *cyp1c1(+3.74), ahr2 (+0.70)*, *ahrra (+2.32)* and *foxq (+2.59)*. In addition, significant changes were observed in genes associated with cartilage development (*mmp9*, *+3.09*; *sox12*, -0.86), blood cell production (*tbx6, +1.35; gatad2b, –0.63*), and oxidative stress *(nfe, +1.76; gstp, +1.79*). The increase in CYP1A and AHR2 proteins were further validated by whole-mount immunohistochemistry (IHC). When co-exposed to GNF, IHC revealed a partial rescue of TBBPA-induced increase of AHR2 and CYP1A protein expressions at both 24 and 72 hpf. Likewise, CH2DCFDA stain showed that GNF partially rescues TBBPA-induced ROS increase at 24 hpf. Finally, at 72 hpf and 120 hpf, o-dianisidine and Alcian Blue staining showed that GNF significantly rescued TBBPA-induced inhibition of blood cell development and craniofacial cartilage structures respectively - both of which are known to be dependent on AHR2 signaling. **Conclusion:** This study demonstrates that TBBPA disrupts cartilage development, blood cell development, and oxidative stress through AHR2-dependent signaling. Since AHR pathway is involved in various developmental and metabolic functions, our work establishes a mechanistic link between environmental exposure, developmental toxicity, and potential health risks. **Future work:** Future studies will study the role of AHR2 in metabolism, oxidative stress and lipid transport by pharmacological and gene editing approaches.

Protecting Predators: A Non-Lethal Framework for Toxicological Risk Assessment in Sharks

Paige Powell
Clemson University

Sharks play a key role in the health and balance of marine ecosystems. As apex predators, they are especially vulnerable to the bioaccumulation of contaminants such as mercury and per and polyfluoroalkyl substances (PFAS), which impact neurological, reproductive, and hepatic function. PFAS levels in estuarine systems are expanding rapidly, while mercury continues to be a global concern due to industrial activity, fossil fuel

combustion, and legacy contamination. Estuaries serve as breeding and nursing grounds for many shark species, making them an area of concern for contaminant exposure. Accurate toxicant concentrations and effective conservation strategies are limited by the lack of non-lethal methods to sample contaminant sensitive tissues, such as the brain, gonads, and liver. We aim to fill this gap by developing a physiologically based pharmacokinetic (PBPK) model using minimally invasive and non-lethal blood and muscle samples to predict contaminant concentrations in specific target tissues. We plan to focus on two coastal species in South Carolina: the finetooth shark (*Carcharhinus isodon*), which has a status of near threatened, and the sandbar shark (*Carcharhinus plumbeus*), which is listed as endangered by the International Union for Conservation of Nature (IUCN). These two species differ in diet and life history traits, making them ideal models for understanding the variability in contaminant exposure. Using species-specific data on various ages, sex, and diets, this model will serve as a scalable, non-lethal tool for evaluating toxicological risk assessment in sharks. We aim to expand the framework of this model to critically endangered species, where internal tissues cannot be legally or ethically obtained. This will advance conservation science, support evidence-based management decisions, and improve protection for shark species, while minimizing harm to vulnerable populations. During summer of 2025, blood and muscle samples were collected in collaboration with Bryan Frazier and his shark research team at South Carolina Department of Natural Resources (SCDNR) using catch-and-release techniques. A subset of specimens' opportunistic organ samples obtained from incidental mortality were collected to facilitate model calibration. Mercury concentrations were quantified by thermal decomposition-amalgamation atomic absorption spectrophotometry. Preliminary data from current organ-specific mercury analysis has shown variability in mercury concentrations in blood, muscle, liver, spleen, stomach, and brain in neonate finetooth sharks, with concentrations being highest in the muscle followed by the liver. On-going studies will analyze (1) PFAS concentrations using high performance liquid chromatography coupled with tandem mass spectrophotometry, targeting a suite of congeners known to be environmentally relevant in marine ecosystems; (2) stable isotope analysis to characterize diet and trophic position to inform model parameterization; and (3) total cardiac output and regional blood flow rate to sensitive organs utilizing doppler ultrasound. Through empirical data from blood, muscle, and opportunistically collected internal tissues, we will develop a preliminary PBPK model that is tailored to shark physiology. This initial phase model will allow us to test core assumptions, refine the model structure, and identify key data gaps.

Polymer-Specific and Time-Dependent Toxicity of Textile-Derived Microfibers in Fish Gill Cells

Beverly Thomas
Auburn University

Background. The rise of fast fashion has driven synthetic fiber production to unprecedented levels, with textile-derived micro- and nanofibers (MNFs) entering aquatic systems through laundering and leaching from landfills. These fibers disperse globally, aided by atmospheric circulation, and their elongated shapes enhance environmental persistence. Despite this widespread fiber contamination, most toxicological studies still rely on spherical, pristine plastic particles, overlooking the fact that weathered fibers undergo photooxidation, sink in water, sorb co-contaminants, and exhibit altered bioaccumulation potential. **Methods**. We evaluated the cytotoxicity of **polyester** (PL; mean length 77.03 ± 53.70 µm, width 19.20 ± 12.49 µm), **nylon 6,6** (PA; mean length 88.40 ± 16.78 µm, width 25.95 ± 16.82 µm), **nylon 6,6 oligomers** (PA_o), and **cotton,** a natural fiber**,** (CO; mean length 90.68 ± 50.63 µm, width 20.42 ± 15.78 µm) in rainbow trout gill cells (RTGill-W1) following OECD Test Guideline 249. RTGill-W1 cells were routinely cultured in L-15 medium with 10% FBS and 0.5% gentamicin at 20°C. Fibers were collected from laundering wastewater, ultrasonicated to simulate mechanical weathering and reduce size, and subsequently characterized. Polymer identity was confirmed by attenuated total reflectance Fourier-transform infrared spectroscopy (ATR-FTIR), thermogravimetric analysis (TGA), and scanning electron microscopy (SEM) while inductively coupled plasma mass spectrometry (ICP-MS) was used to detect trace metals. Before exposure, fibers were incubated in fetal bovine serum to allow protein corona formation. Cells were then exposed to four concentrations (0.1, 1, 10, and 100 µg/mL for fibers; 0.065, 0.65, 6.5, and 65 ng/mL for PA_O) for 24, 48, and 72 h. The two lower concentrations reflect environmentally relevant levels, while the higher concentrations fall within hazardous range. Sodium dodecyl sulfate (0.5 mM) and tert-butyl hydroperoxide

Sponsors:

(1 mM) served as positive controls. Cellular health was assessed using OECD-aligned assays: **metabolic activity** (Alamar Blue), **esterase function** (CFDA-AM), and **lysosomal integrity** (Neutral Red), with data normalized to untreated controls. **Results**. Distinct polymer-specific patterns were observed. Following 72h exposure, all polyester (PL) treatment groups showed suppressed cellular metabolism measured by Alamar Blue, with the strongest decline at 1 µg/mL (**$p < 0.001$**). Lysosomal destabilization was also significant after 72 h for 0.1 and 100 µg/mL (**$p < 0.01$**). ICP-MS revealed Cu, Cr, and Zn in nylon 6,6 (PA) fibers and Zn, Ni, Cr, and Ag in cotton (CO). Fibers carrying Cu/Cr/Zn caused significant metabolic suppression at the lowest doses, which may be indicative of redox-active metal–driven mitochondrial dysfunction. PA produced immediate metabolic suppression across doses, with the strongest effects at 72 h: both the 0.1 µg/mL and 100 µg/mL groups showed highly significant reductions in metabolic activity (**$p < 0.001$**) and lysosomal destabilization was also evident at these doses **($p < 0.01$**). Nylon 6,6 oligomer (PA_O) displayed non-linear responses; low concentrations transiently decreased metabolism and esterase activity at 24 h, but following 48–72 h exposure, all doses converged on metabolic suppression, with lysosomal damage highly significant at 6.5 ng/mL (**$p < 0.0001$**). CO caused more linear declines, with significant reductions in esterase, metabolism, and lysosomal activity by 48–72 h. A pronounced lysosomal drop observed at 10 µg/mL, associated with Ag/Ni presence, was detected and may reflect lysosomal destabilization, though this cannot be definitively attributed to the co-contaminants ($p < 0.001$). Lysosomal integrity emerged as the most sensitive indicator of sustained MNF and oligomer induced stress. **Conclusion**. These findings demonstrate that fiber chemistry shapes distinct cytotoxicity that is not captured by traditional spherical microplastic models. The consistent sensitivity of lysosomal integrity across polymers underscores its utility as a sentinel endpoint for fiber-induced stress. By showing that both synthetic (polyester, nylon, nylon oligomer) and natural textile fibers drive significant, polymer-specific cellular effects (including highly significant reductions at environmentally relevant concentrations, **$p < 0.001$**), this work highlights the urgent need for fiber- and polymer-aware testing frameworks. Incorporating such approaches into OECD-aligned protocols will strengthen ecological risk assessments and better inform regulatory decisions on micro- and nanoplastics.

Persistently Distinct PPCP Contaminant Profiles in the Lake Huron–Lake Erie Corridor: A Multi-Year NMDS Study

Emma VanderMeulen
University of Florida

Background and Purpose: The Lake Huron to Lake Erie corridor (HEC) is a section of the Great Lakes between Michigan and Canada. It is an important shipping route along with a diverse habitat for wildlife, housing the only International Wildlife Refuge in North America. The corridor is the drinking water source for up to 4 million people in the region. Previous studies conducted within the HEC have consistently found the emerging contaminant class of pharmaceuticals and personal care products (PPCPs) at ng/L levels. Researchers have shown that PPCPs have endocrine-disrupting potential and could influence the prevalence of antibiotic-resistant genes (ARGs) in the environment. PPCPs can cause negative health outcomes in aquatic species and in humans who engage in recreational activities or consume exposed species from the water. As PPCPs are such a large class and rarely found alone it can be difficult to capture the impact of these mixtures. It is important for risk assessments to consider what kinds of PPCPs are present in a habitat and how that mixture influences health overall. This study uses non-metric multidimensional scaling (NMDS) to identify PPCP contaminant profiles that persist year after year and can represent the influence of mixtures of many PPCPs. **Methods:** Surface water samples were collected from 14 sites in or near the HEC in June 2022, May 2023, May 2024, and May 2025 expanding on previous analysis of samples from this region by Baker et al., 2022. Not all sites were sampled every year. Locations were chosen based on proximity to anthropogenic factors, including tributaries, that can influence water quality. NMDS analysis followed by beta dispersion and PERMANOVA were used to determine significant contaminant groups. **Results:** To assess contaminant composition of sites sampled in 2025, the data was first log-transformed followed by Z-score standardization. Bray–Curtis distance matrix was calculated prior to hierarchical clustering and NMDS. A low stress value of (0.06) indicated a good ordination fit and reliable representation of the multivariate relationships between site contaminant profiles. No significant differences were found in within-cluster beta dispersion, indicating that the assumption of homogeneity of multivariate spread

essential for PERMANOVA was reasonably met. Subsequently, PERMANOVA was significant for differences between cluster compositions ($F = 7.61$, $R^2 = 0.58$, $p = 0.001$), which indicates clusters were significantly different from one another based on the site's contaminant multivariate profiles. Based on the non-significant beta-dispersion results, these differences likely reflect genuine differences in the cluster centroids. Historical data from 2022-2024 was compiled and analyzed using the same methods applied to the 2025 data, however with fewer variables as fewer analytes were tested for those years. The historical plot also had a low stress value (0.07), non-significant beta-dispersion, and significant PERMANOVA ($F = 13.10$, $R^2 = 0.71$, $p = 0.001$). Both plots identified an urban cluster, an agricultural cluster, and an upstream/intake cluster. The historical plot identified a fourth highly industrial cluster. **Conclusion:** Identifying consistent contaminant profiles will be a valuable method for risk assessments of PPCPs in the environment. By establishing these profiles, researchers and city planners can represent the impact of a complex mixture of PPCPs with a single contaminant profile designation. Consistent profiles in the HEC were identified across the two plots including urban, agricultural, and upstream/intake. Future studies can link health outcomes associated with these profiles and use the information to better inform community risk assessments.

Sponsors:

UL Research Institutes | Chemical Insights

Department of BIOLOGICAL SCIENCES Clemson University

College of SCIENCE

Postdoctoral Poster Abstracts

Interpretable machine learning reveals key drivers of inorganic nanoparticle cytotoxicity

Chi-Yun Chen
University of Florida

Research Background and Purpose: Inorganic nanoparticles hold significant promise for medical therapies and cosmetic applications due to their stability and tunable compositions. Although numerous cell-based assays have been conducted, the extent of cell-associated nanoparticle levels remains poorly characterized, largely due to variations in nanoparticle preparation and experimental design, especially for less common materials. This hampers the comparison of cytotoxicity profiles across studies. To capture the interactive effects of multiple variables on nanoparticle cytotoxicity, we applied machine-learning techniques to analyze thousands of cell viability profiles and identify the most influential factors driving cytotoxic responses. Our novelty lies in the use of an expanded dataset spanning noble metals, metal oxides, silica, and other inorganic nanoparticle types, enabling generalized, accurate, and physically consistent predictions through feature-based machine learning. **Methods:** We curated a comprehensive dataset covering 19 core materials and 141 cell types (80% human), drawn from three primary publications, yielding 9249 entries. Of these, 6016 entries with quantitative viability values were used for regression modeling. In total, 15 data-driven features were finalized, supplemented with two domain knowledge-based descriptors, molecular weight and electronegativity, calculated using Python packages. Key data challenges (noise, missing values), feature selection, and feature scaling were addressed to reduce computational complexity prior to modeling. Classification and regression models were constructed using tree-based algorithms (CatBoost, Gradient Boost, Random Forest, XGBoost), K-Nearest Neighbors (KNN), Support Vector Machine (SVM), and neural networks. Model hyperparameters were optimized through 5-fold nested cross-validation, and the best models were identified based on multiple performance metrics. **Results:** The CatBoost classifier delivered the best classification performance, achieving 0.89 accuracy, 0.85 precision, 0.83 recall, and 0.95 area under the curve (AUC) on the test set with 255 reduced one-hot features. Its confusion matrix revealed only 193 misclassifications, highlighting its robustness. For regression, Gradient Boost achieved 0.76 ± 0.03 adjusted R^2, 12.2 ± 0.7% weighted mean absolute percentage error (WMAPE), and 14.2 ± 1% root mean squared error (RMSE) with 228 reduced one- hot features. SHAP analysis identified exposure concentration and electronegativity as the most influential features across models. Notably, zeta potential ranked among the top three in regression, whereas hydrodynamic diameter emerged as the second most influential predictor in classification models, showing a negative association with cytotoxicity risk. These descriptors are central to nanoparticle design and provide valuable mechanistic insight into how cells respond to nanoparticles in real-world contexts. **Conclusions:** This study reports a robust machine learning model that provides accurate and generalizable cytotoxicity predictions across various inorganic nanoparticles based on their physicochemical properties and experimental design factors. This approach not only highlights the promise of machine learning modelling effectively deciphering complex nanoparticle–cell interactions, but also reveals critical design insights to guide safer nanoparticle application.

Sex-Dependent Disruption of Adiposity and Vitamin D_3 Metabolism by Microbiome-Derived Delta-Valerobetaine in Aged Mice

Ho Young Lee
Emory University

Aging is characterized by metabolic changes along with alterations in overall adiposity and in lipid-associated signaling molecules, including vitamin D_3 - features that are closely linked with greater susceptibility to adverse health outcomes. Microbiome-derived metabolites have recently been recognized as regulators of host metabolism, yet their roles in age-related dysfunction remain poorly defined. Dietary exposure to delta-valerobetaine (VB), a gut microbiome metabolite previously shown to promote adiposity in young mice under high-fat diet conditions, has not been investigated in the context of aging. To evaluate the impact of chronic VB exposure, aged C57BL/6J mice (~21 months old) were provided VB-supplemented drinking water (1.62 mM) or

vehicle for 12 weeks. Body weight, adipose depot distribution, hepatic and plasma triglycerides, high-resolution metabolomics, and expression of cytochrome P450 enzymes central to vitamin D_3 metabolism were assessed. VB exposure resulted in a significant increase in body weight and in the ratio of white adipose tissue (WAT) to brown adipose tissue (BAT) in aged female mice, whereas no changes were observed in males. Despite this adiposity expansion, hepatic steatosis and systemic triglycerides were not elevated, suggesting preferential lipid storage within WAT depots. High-resolution metabolomics of liver tissue detected 13,443 metabolic features, with 738 significantly altered ($p < 0.05$) in VB-exposed females. Two-way HCA demonstrated distinct separation of VB and control groups, with pathway enrichment analysis identifying perturbations in fatty acid metabolism, bile acid biosynthesis, prostaglandin signaling, and vitamin D_3 metabolism. Targeted analysis confirmed reduced hepatic 25-hydroxyvitamin D_3 and plasma 1,25-dihydroxyvitamin D_3, while precursor vitamin D_3 and inactivated metabolites remained unchanged. Expression of CYP2R1, CYP27B1, CYP27A1, and CYP3A11 did not differ, indicating that VB decreases vitamin D_3 bioavailability independent of canonical hydroxylase gene regulation. Metabolomics analysis of kidney tissue further revealed perturbations in the carnitine shuttle, vitamin D_3 metabolism, bile acid synthesis, vitamin E metabolism, and saturated fatty acid β-oxidation. Together with the hepatic pathways identified, these results suggest that VB exposure alters multiple organ systems central to lipid handling, including mitochondrial fatty acid oxidation, lipid absorption, antioxidant metabolism, and vitamin D regulation. Female-specific effects may reflect microbiota composition, as VB-producing genera (Lactobacillus, Bifidobacterium) are more abundant in females, leading to higher baseline VB. Increased WAT depots can sequester vitamin D_3 intermediates, reducing circulating levels, consistent with clinical observations in obesity. Collectively, these findings demonstrate that VB exposure alters systemic metabolic networks across liver and kidney, promotes adiposity, and reduces vitamin D_3 intermediates in aged female mice. Taken together, the results identify delta-valerobetaine as a microbiome-derived metabolite that drives sex-specific metabolic dysfunction during aging.

Cadmium Promotes Extracellular Mer Generation via ADAM17, Impairing Efferocytosis and Contributing to the Pathogenesis of Emphysema

Gopikrishnan Mani
University of Alabama at Birmingham

Objective: Cadmium (Cd) is a harmful environmental pollutant commonly present in water, air, soil and industrial activity. Cd accumulated in the lungs and other organs may inevitably affect intracellular signaling, resulting in chronic inflammation, COPD, and emphysema. Our objective of this study was to determine the mechanisms of Cd induced impaired efferocytosis (phagocytic clearance of apoptotic cells) leading to chronic inflammation and lung injury. **Methods**: Mouse alveolar macrophage cells treated with cadmium, and were assessed for their efferocytosis ability. The cell lysates were used for immunoblotting for the efferocytosis protein MerTK, and ADAM17. C57BL/6 mice (8-10 weeks old, both male and female), or $MerTK^{KD}$ were exposed to cadmium and evaluated for immunohistochemical analysis, lung functions, and lung injury at Day 21st. Ex vivo and in situ efferocytosis assays were performed to analyze efferocytosis function in alveolar macrophages of control and cadmium-exposed mice. The effects of ADAM17 inhibitor and soluble Mer treatments were analyzed in control and cadmium-exposed mice. **Results:** Cadmium decreased the efferocytosis index in alveolar macrophages; however, it upregulated MertK expression. Further, we found that Cd treatment led to MerTK shedding by activation of ADAM17. A proteolytic cleavage of Mer generated extracellular form of Mer, which acted as a decoy receptor by binding to Gas6, and inhibited efferocytosis. In vivo studies, we observed that Cd increased sMer levels, ADAM17 activity, and decreased efferocytosis, and caused emphysema. Treatment with ADAM17 inhibitor in vitro and in vivo, decreased extracellular Mer levels and improved efferocytosis index. The intratracheal administration of sMer was pathological itself, and showed decreased efferocytosis index and increased inflammation and emphysema in lungs. The sMer co-treatment with cadmium worsen the inflammation and emphysema and efferocytosis index. Further, we observed that worsening cellular injury, emphysema in $MerTK^{KD}$ mice as compared with $MerTK^{+/+}$ Cd exposed mice. Interestingly, COPD plasma samples showed increase in soluble Mer levels as compared with control subjects. **Conclusion**: Cadmium increases levels of

extracellular Mer and decoy scavenger receptor MerTK for efferocytosis. The anti-efferocytic activity of sMer perpetuates inflammation and causes emphysema.

The effects of trichloroethylene exposure on cognitive behavior in PFF-injected mice

Allie Smith
University of Alabama at Birmingham

Background and Purpose: Trichloroethylene (TCE) is an organic solvent that is commonly used as a metal degreaser and chemical feedstock. Occupational TCE exposure has been associated with an increased risk for developing Parkinson's disease (PD), and epidemiological data demonstrates that TCE exposure can increase the rate of PD progression. Previously published experimental data shows that α-synuclein (αSyn) accumulates in the dopaminergic neurons of animals exposed to TCE. In the αSyn preformed fibril (PFF) model of synuclein-induced neurodegeneration, cognitive deficits, particularly in contextual fear conditioning have also been reported. As the accumulation and spread of αSyn is postulated to be a key driver of cognitive deficits in PD, we hypothesized that TCE exposure in conjunction with αSyn PFFs would provide an advanced experimental model of environmental exposure to assess cognitive phenotypes associated with Parkinson's neurodegeneration. **Methods:** Adult male and female C57BL/6 mice were bilaterally injected in the striatum with 5 µg αSyn monomer or PFFs. Three weeks following injection, mice were exposed to 100 ppm TCE or room air (VEH) via passive inhalation. After 3 months of TCE exposure, the mice were tested in a behavioral battery including the open field test, novel object recognition, Y maze, and catwalk. **Results:** In the open field test, mice exposed to TCE made fewer entries into the center of the field than mice exposed to room air, regardless of αSyn injection ($p=0.0100$). Additionally, during novel object recognition, TCE exposed mice had a greater discrimination index than VEH mice ($p=0.0106$). In particular, PFF TCE mice had a significantly greater discrimination index compared to αSyn monomer VEH controls ($p=0.0149$). However, performance in the Y maze was not significantly affected by αSyn injection or exposure type. In catwalk analyses, TCE exposed mice had a significantly smaller right hind paw area compared to VEH mice ($p=0.0450$), while other paw areas were not affected. **Conclusions:** We conclude that exposure to TCE exposure may increase novelty-seeking behavior that is further emphasized by PFF injection, while TCE alone induces an anxiety-like phenotype. Overall, these data suggest that additional cognitive behavioral tests may be required to fully characterize cognitive effects of TCE in the context of synucleinopathy.